SYNTHESIS, CHARACTERIZATION AND ELECTROCHROMIC PROPERTIES OF CONDUCTING COPOLYMERS OF TEREPHTHALIC ACID BIS-(THIOPHEN-3-YLMETHYL)THIOESTER WITH THIOPHENE AND PYRROLE AND CONDUCTING POLYMER OF 1-(4-FLUOROPHENYL)-2,5-DI(THIOPHEN-2-YL)-1H-PYRROLE

A THESIS SUBMITTED TO
THE GRADUATE SCHOOL OF NATURAL AND APPLIED SCIENCES
OF
MIDDLE EAST TECHNICAL UNIVERSITY

BY

ÖZLEM TÜRKARSLAN

IN PARTIAL FULFILLMENT OF THE REQUIREMENTS
FOR
THE DEGREE OF MASTER OF SCIENCE
IN
CHEMISTRY

MAY 2006

Approval of the Graduate School of Natural and Applied Sciences

Prof. Dr. Canan Özgen
Director

I certify that this thesis satisfies all the requirements as a thesis for the degree of Master of Science.

Prof. Dr. Hüseyin İşçi
Head of Department

This is to certify that we have read this thesis and that in our opinion it is fully adequate, in scope and quality, as a thesis for the degree of Master of Science.

Prof. Dr. Levent Toppare
Supervisor

Examining Committee Members

Prof. Dr. Leyla Aras (METU, CHEM)

Prof. Dr. Levent Toppare (METU, CHEM)

Prof. Dr. Teoman Tinçer (METU, CHEM)

Prof. Dr. Mustafa Güllü (Ankara Univ, CHEM)

Dr. Senem Kıralp (METU, CHEM)

I hereby declare that all information in this document has been obtained and presented in accordance with academic rules and ethical conduct. I also declare that, as required by these rules and conduct, I have fully cited and referenced all material and results that are not original to this work.

Name, Last name :

Signature :

ABSTRACT

SYNTHESIS, CHARACTERIZATION AND ELECTROCHROMIC PROPERTIES OF CONDUCTING COPOLYMERS OF TEREPHTHALIC ACID BIS-(THIOPHEN-3-YLMETHYL)THIOESTER WITH THIOPHENE AND PYRROLE
AND
CONDUCTING POLYMER OF 1-(4-FLUOROPHENYL)-2,5-DI(THIOPHEN-2-YL)-1*H*-PYRROLE

Türkarslan, Özlem
M.S., Department of Chemistry
Supervisor: Prof. Dr. Levent Toppare

May 2006, 92 pages

Terephthalic acid bis-(thiophen-3-ylmethyl)thioester (TTMT) was synthesized via the reaction of thiophen-3-ylmethanethiol with terephthaloyl dichloride. Nuclear magnetic resonance (^{1}H-NMR) and Fourier transform infrared (FTIR) spectroscopies were utilized for the characterization of the monomer. This 3-functionalized thiophene monomer was polymerized in the presence of thiophene (Th) and pyrrole (Py) upon constant potential application in acetonitrile/tetrabutylammonium tetrafluoroborate (TBAFB). The resulting copolymers were characterized via cyclic voltammetry (CV),

FTIR, differential scanning calorimetry (DSC), scanning electron microscopy (SEM), four-probe technique conductivity measurement and UV-Vis spectroscopy. Spectroelectrochemical analysis of P(TTMT-co-Th) revealed π to π* transition at 476 nm with a band gap of 2.0 eV whereas, λmax and Eg were found as 375 nm and 2.4 eV for P(TTMT-co-Py), respectively. Dual type electrochromic devices (ECDs) of P(TTMT-co-Th) and P(TTMT-co-Py) with poly(3,4-ethylenedioxythiophene) (PEDOT) were constructed. Spectroelectrochemistry, switching ability, open circuit memory and stability of the devices were examined by UV-Vis spectroscopy and cyclic voltammetry. The device P(TTMT-co-Th)/PEDOT switches between brown and blue upon application of 0.0 V and +2.6 V, respectively with 11% optical contrast and 1.1 s as the switching time. On the other hand, P(TTMT-co-Py)/PEDOT ECD exhibits greenish yellow, grayish red and blue colors with the application of -2.4 V, 0.0 V and +0.8 V, respectively and the contrast between extreme potentials was 17.5% with a switching time of 1.6 s.

1-(4-Fluorophenyl)-2,5-di(thiophen-2-yl)-1*H*-pyrrole (FPTP) was synthesized and polymerized both chemically and electrochemically. Several analytical techniques, such as NMR, FTIR, CV, gel permeation chromatography (GPC), four-probe conductivity measurement, SEM were utilized when applicable. Spectroelectrochemistry experiments reflected a π to π* transition at 398 nm with a band gap energy of 1.94 eV for the polymer. A dual type electrochromic device (ECD) of PFPTP and poly(3,4-ethylenedioxythiophene) (PEDOT) was constructed. The device switches between yellowish brown and blue upon application of –0.8 V and +1.1 V, respectively. Optical contrast was calculated as 19.4% with a switching time of 1.4 s at maximum contrast point.

Keywords: Conducting polymers, organic electrochromics, electrochromic devices

ÖZ

TEREFTALİK ASİT BİS-(TİYOFEN-3-İLMETİL) TİOESTERİN İLETKEN KOPOLİMERLERİNİN
VE
1-(4-FLOROFENİL)-2,5-Dİ(TİYOFEN-2-İL)-*1H*-PİROLÜN İLETKEN POLİMERİNİN
SENTEZİ, KARAKTERİZASYONU, ELEKTROKROMİK ÖZELLİKLERİ

Türkarslan, Özlem
Yüksek Lisans, Kimya Bölümü
Tez Yöneticisi: Prof. Dr. Levent Toppare

Mayıs 2006, 92 sayfa

Tereftalik asit bis-(tiyofen-3-ilmetil)tioester (TTMT) tiyofen-3-ilmetantiol ile tereftaloil diklorürün tepkimesiyle sentezlenmiştir. Bu monomerin tiyofen ve pirol ile kopolimerleri sabit potansiyel uygulanarak asetonitril/tetrabütilamonyum tetrafloroborat ortamında sentezlenmiştir. P(TTMT-co-Th)nin spektroelektrokimyasal analizi sonucu π-π* geçişi 476 nm'de gözlenmiş bant aralığı 2.0 eV hesaplanmıştır, öte yandan P(TTMT-co-Py)nin λmax ve Eg değerleri sırasıyla 377 nm ve 2.4 eV bulunmuştur. P(TTMT-co-Th) ve P(TTMT-co-Py)nin poly(3,4-etilendioksitiyofen) (PEDOT) ile dual tip elektrokromik cihazları yapılmıştır. P(TTMT-co-

Th)/PEDOT cihazı 0.0 V uygulandığında kahverengi, +2.6 V uygulandığında ise mavi renkli olmaktadır, optik kontrast %11, değişim zamanı ise 1.1 saniyedir. P(TTMT-co-Py)/PEDOT cihazında ise sarımtırak yeşil, grimsi kırmızı ve mavi renkler sırasıyla –2.4 V, 0.0 V ve +0.8 V uygulandığında gözlemlenmiştir, bu cihazın optik kontrastı %17.5 değişim zamanı ise 1.6 saniyedir.

1-(4-Florofenil)-2,5-di(tiyofen-2-il)-1*H*-pirol (FPTP) sentezlenmiş, kimyasal ve elektrokimyasal yollarla polimerleştirilmiştir. Spektroelektrokimya deneyleri sonucu π-π* geçişinin 398 nm'de olduğu gözlemlenmiş, bant aralığı ise 1.94 eV olarak hesaplanmıştır. P(FPTP)nin PEDOT ile dual tip elektrokromik cihazı yapılmıştır. Bu cihaz –0.8 V uygulandığında sarımtırak kahverengi +1.1 V uygulandığında ise mavidir. Optik kontrast %19.4, değişim zamanı ise 1.4 saniye olarak hesaplanmıştır.

Anahtar sözcükler: İletken polimerler, organik elektrokromikler, elektrokromik cihazlar

TO MY FAMILY AND BOSS

ACKNOWLEDGMENTS

I would like to express my greatest appreciations to my supervisor Prof. Dr. Levent Toppare for his extraordinary guidance, encouragements, advice, criticism, patience and friendship.

I would like to thank Prof. Dr.Mustafa Güllü, Prof. Dr. İdris Mecidoğlu Akhmedov, Prof. Dr. Cihangir Tanyeli for their help in the synthesis of the monomers.

I gratefully thank Prof. Dr. Metin Balcı for his valuable comments on the NMR spectra.

I owe great thanks to Dr. Elif Şahin, Pınar Şanlı, Metin Ak, Dr. Senem Kıralp, Dr. Ertuğrul Şahmetlioğlu for their help, technical support and answering my questions anytime in the laboratory, besides their kind friendship.

I am grateful to all my lab-mates in our research group for their kind friendship and I would like to express my special thanks to Simge Tarkuç, Başak Yiğitsoy, Serhat Varış, Balam Balık, Yusuf Nur for their endless amity.

Finally I would like to thank to my family for always being there for me.

TABLE OF CONTENTS

LIST OF FIGURES

FIGURES

LIST OF TABLES

TABLES

ABBREVIATIONS

TMTT	Terephthalic acid bis-(thiophen-3-ylmethyl) thioester
(TTMT-co-Th)	Poly(terephthalic acid bis-(thiophen-3-ylmethyl)thioester-co-thiophene)
(TTMT-co-Py)	Poly(terephthalic acid bis-(thiophen-3-ylmethyl)thioester-co-pyrrole)
Th	Thiophene
Py	Pyrrole
FPTP	1-(4-Fluorophenyl)-2,5-di(thiophen-2-yl)-1*H*-pyrrole
P(FPTP)	Poly(1-(4-fluorophenyl)-2,5-di(thiophen-2-yl)-1*H*-pyrrole)
DTBD	1,4-di (2-thienyl)-butane-1,4-dione
EDOT	3,4-Ethylenedioxythiophene
PEDOT	Poly(3,4-ethylenedioxythiophene)
AN	Acetonitrile
TBAFB	Tetrabutylammonium tetrafluoroborate
BFEE	Boron trifluoride diethyl etherate
NBS	N-Bromo succinimide
TEA	Triethylamine
PMMA	Poly(methymethacrylate)
PC	Propylene carbonate
NMR	Nuclear Magnetic Resonance

FTIR	Fourier Transform Infrared Spectrometer
CV	Cyclic Voltammetry
DSC	Differential Scanning Colorimetry
SEM	Scanning Electron Microscopy
GPC	Gel Permeation Chromatography
CP	Conducting Polymer
ECD	Electrochromic Device
HOMO	Highest Occupied Molecular Orbital
LUMO	Lowest Unoccupied Molecular Orbital
E_g	Band Gap Energy
CIE	La Commission Internationale de l'Eclairage
L a b	Luminance, hue, saturation

CHAPTER I

INTRODUCTION

1.1 Conducting Polymers

Conducting polymers (CPs) are the new generation of polymers containing π-electron backbone responsible for their conducting properties. Those organic polymers, named as 'synthetic metals', possess the electrical, electronic, magnetic and optical properties of a metal while retaining the ease of processibility associated with an ordinary polymer. Conducting polymers are still intensely investigated from different perspectives. Studies of the electronic structure of the neutral and doped conjugated polymers have opened potential application areas.

1.1.1 Historical Review of Conducting Polymers

A first conducting polymer was the inorganic polymer sulfur nitride, $(SN)_x$, which was discovered in 1973, showed properties very close to those of a metal. The room temperature conductivity of $(SN)_x$ was of the order of 10^3 S/cm [1]. As a comparison, copper has a conductivity of 1×10^6 S/cm, and polyethylene, 10^{-14} S/cm. Although its explosive nature prevented it from becoming commercially important, it proved the existence of highly conducting polymers, and led to the discovery of an entirely new class of conducting polymers.

The Nobel Prize in chemistry for the year 2000 went to Alan Heeger, Alan MacDiarmid, and Hideki Shirakawa "for the discovery and development of electrically conducting polymers." The three winners launched that if the polymer backbone contained alternating single and double bonds, and electrons are either removed through oxidation or introduced through reduction, the polymer can conduct electricity. Normally the electrons in the bonds remain localized and cannot carry an electric current, but when the team "doped" the material with strong electron acceptors such as iodine, the polymer began to conduct nearly as well as a metal, with conductivity 10^{11} times higher than pure polyacetylene (PA) [2,3]. Although polyacetylene exhibits a very high conductivity in the doped form, the material is not stable to oxygen or humidity and is obstinate. For these reasons, much work has been devoted to synthesizing soluble and stable polyacetylenes [4,5]. Unfortunately, these substituted derivatives exhibit electrical conductivities that are much lower than the parent polymer. The discovery of polyacetylene led to the search for new structures that could lead to new and improved polymer properties. In 1980's polyheterocyles (Figure 1.1), which were more air stable than polyacetylene, due to lower polymer oxidation potential, were first developed. New classes of conducting polymers include polythiophene (PTh), polyfuran, polypyrrole (PPy), poly(p-phenylene) (PPP), poly(p-phenylene vinylene) (PPV), poly(paraphenylene sulphide) (PPS) and polyaniline (PAn). In Figure 1.2 conductivities and stabilities of some of these polymers were shown. Even if none have exhibited higher conductivity than polyacetylene, these polymers have been helpful in designing new monomers functionalized with Th, Py, etc. that are soluble and stable. By adding various side groups, electron donating or withdrawing, to the polymer backbone, soluble derivatives can be prepared; in addition, the electronic structure of the material can be manipulated.

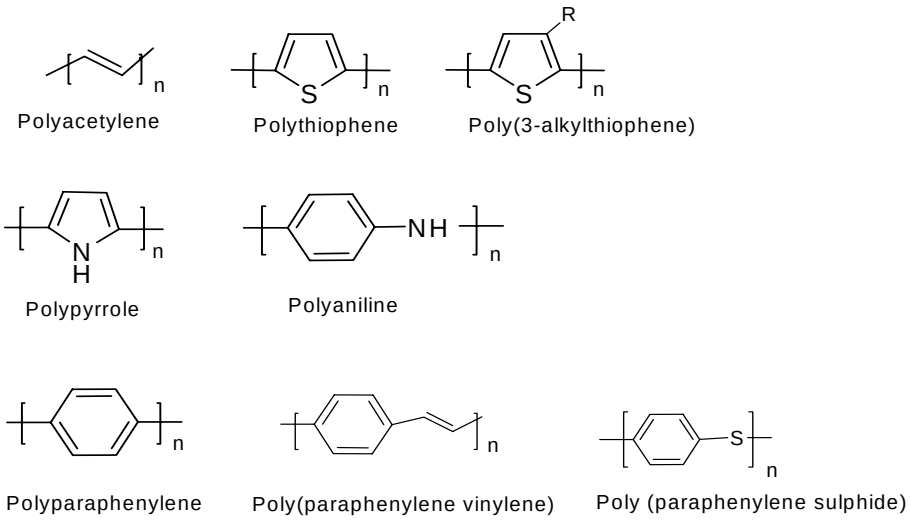

Figure 1.1 Structures of some common conducting polymers

POLYMER	CONDUCTIVITY (Ω^{-1} cm^{-1})	STABILITY (doped state)	PROCESSING POSSIBILITIES
Polyacetylene	10^3 - 10^5	poor	limited
Polyphenylene	1000	poor	limited
PPS	100	poor	excellent
PPV	1000	poor	limited
Polypyrroles	100	good	good
Polythiophenes	100	good	excellent
Polyaniline	10	good	good

Figure 1.2 Conductivities and stabilities of some common conducting polymers

1.2 Band Theory and Conduction Mechanism in Conducting Polymers

The movement of charge carriers such as electrons and holes through a medium (metal, polymer, etc.) under influence of an electric field is named as electronic conduction. Thus, the number of charge carriers available and their ability to move through the medium characterize the conductivity of the medium. In Figure 1.3 conductivities of some metals and polymers were displayed.

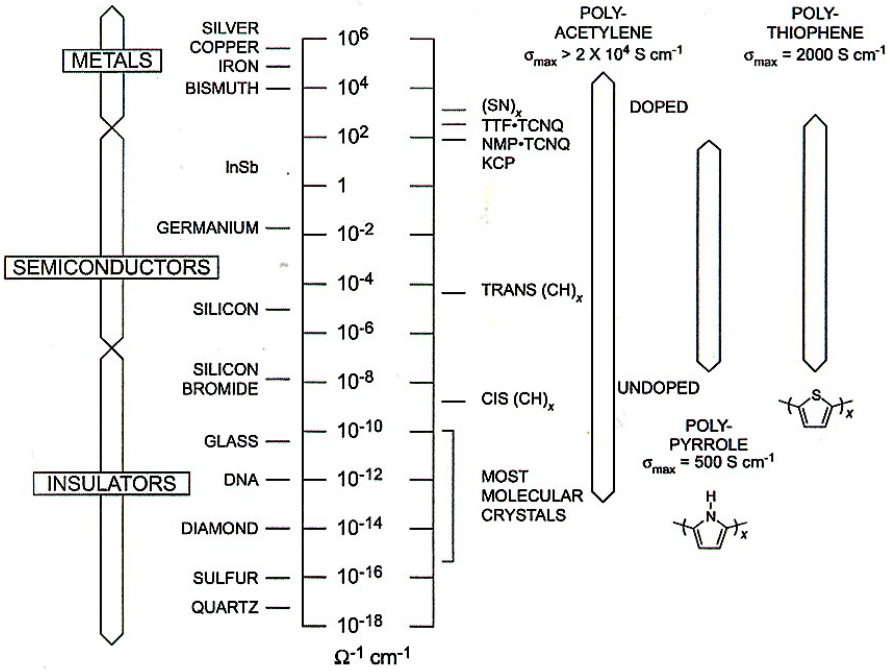

Figure 1.3 Conductivities of some metals, semiconductors and insulators

The electronic configuration of conjugated polymers is totally different than that of saturated polymers (in which all of the four valence electrons of carbon are used up in covalent bonds). In conjugated polymers, the chemical bonding leads to one unpaired electron (the π electron) per carbon atom. Moreover, π bonding, in which the carbon orbitals are in the sp^2p_z configuration and in which the orbitals of successive carbon atoms along the backbone overlap, leads to electron delocalization along the backbone of the polymer. This electronic delocalization provides the 'highway' for charge mobility along the backbone of the polymer chain [6].

In conducting polymers, as well the electronic conductivity is explained using the Band Theory.

1.2.1 Band Theory

A useful way to visualize the difference between conductors, insulators and semiconductors is to plot the available energy levels for electrons in the materials. Instead of having discrete energies as in the case of free atoms, the available energy states form bands. The highest energy band containing electrons is called the valence band; the next higher empty band is called the conduction band. Conduction process depends on whether or not there are electrons in the conduction band. In insulators the electrons in the valence band are separated by a large gap from the conduction band, in conductors like metals the valence band overlaps the conduction band, and in semiconductors there is a small gap between the valence and conduction bands that thermal or other excitations can bridge the gap (Figure 1.4). When electrons are excited to higher energy levels, the holes (electron vacancies) are left behind in the occupied portion of the band. In conductors, both electrons and holes are free to move.

Other elements that are not semiconductors in the pure state can be modified by adding a small amount of another element with energy levels close to those of the host to make doped semiconductors. Doping can be thought of as replacing a few atoms in the original element with atoms having either more or fewer electrons. If the added material has more electrons in the valence shell than the host material, the result is a ‘n-type semiconductor’. Phosphorous is an example in a silicon host, with five electrons compared with four electrons in silicon. If the added material has fewer electrons than the host, it adds positive holes and the result is a ‘p-type semiconductor’. Aluminum is a p-type dopant in a silicon host with three electrons. In conclusion, in n-type material there are electron energy levels near the top of the band gap so that they can be easily excited into the conduction band, whereas, in p-type material, extra holes in the band gap allow excitation of valence band electrons, leaving mobile holes in the valence band (Figure 1.5). In a semiconductor, ‘Fermi level’ (E_f), which is the energy at which electron is

equally likely to be in each of the two levels, is near the middle of the band gap. This level may be raised or lowered upon n-type doping or p-type doping, respectively [7].

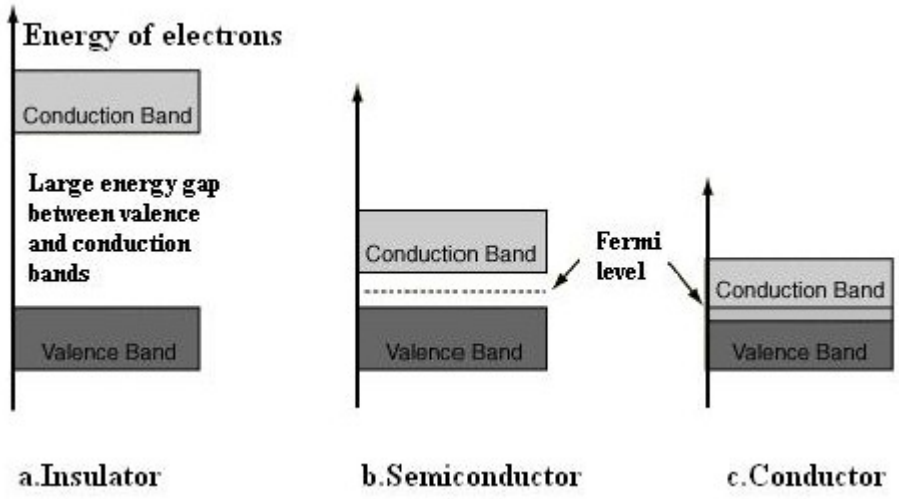

Figure 1.4 Band structures of (a) insulator, (b) semiconductor, (c) conductor

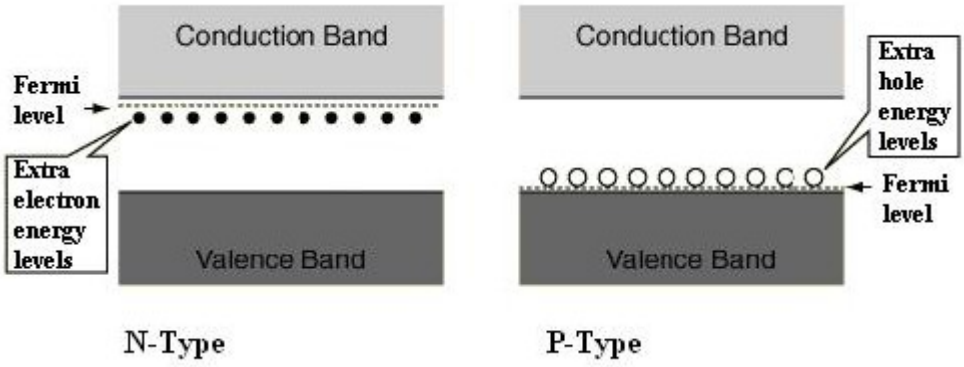

Figure 1.5 Semiconductor bands for n-type semiconductor and p-type semiconductor

In conjugated polymers, e.g. polyacetylene, $(-CH=CH-)_n$, the π band is divided into π and π* bands. Since each band can hold two electrons per atom

(spin up and spin down), the π band is filled, as a consequence π* band is empty. The energy difference between π band (highest occupied state, valence band) and π* band (lowest unoccupied state, conduction band) is called band gap energy and symbolized as 'Eg'. Conjugated polymers are typically semiconductors and the doping process modifies their electronic structure by producing new states in the band gap and makes them conducting. When a polymer conducts, the electrical charge travels through the polymer. The overall mobility of electrical charges is dependent on how easily the charges move inside the polymer. It depends on the movement of electrical charges along the polymer chain, called intra-chain movement, and also jumping from one chain to another, called inter-chain movement. Therefore, the overall mobility of charges is related to intra-chain and inter-chain mobilities.

1.2.2 Conduction Mechanism

1.2.2.1 Doping

The concept of doping is the unique, central, underlying, and unifying theme, which distinguishes conducting polymers from all other types of polymers [8]. Doping a polymer not only means oxidizing or reducing the polymer to provide electrons or create holes in the bands but also generates defects in the polymer's structural chain without destroying the chain. These defects in the polymer, are the charge carriers and can be radicals, anions, cations or combinations of these. They are called solitons, polarons, bisolitons and bipolarons. Figure 1.6 shows the structure of these charge carriers.

Polypyrrole, well known conducting polymer, can be used as illustration (Figure 1.7). Upon removal of an electron from the chain, a radical cation or polaron is formed. A polaron has both a bonding and an antibonding state and these states come in the mid gap with the bonding state holding the unpaired electron. When another electron is removed another polaron is created, as a result the mid gap states are unfilled since both of the electrons form a new π

bond which will reenter the HOMO band. Further oxidation creates more polarons on the chain and the rearrangement of these species gives rise to a carbodication species or bipolarons. As the number of bipolarons formed increases so does the density of the bipolaron states in the mid gap. When the number of states becomes large enough, bipolaron bands are formed just as the valence and conduction bands are formed. These new bands can be considered as 'ladder', which enables electrons to jump from lower energy states to higher energy states. This is what gives conducting polymers their semiconductor properties.

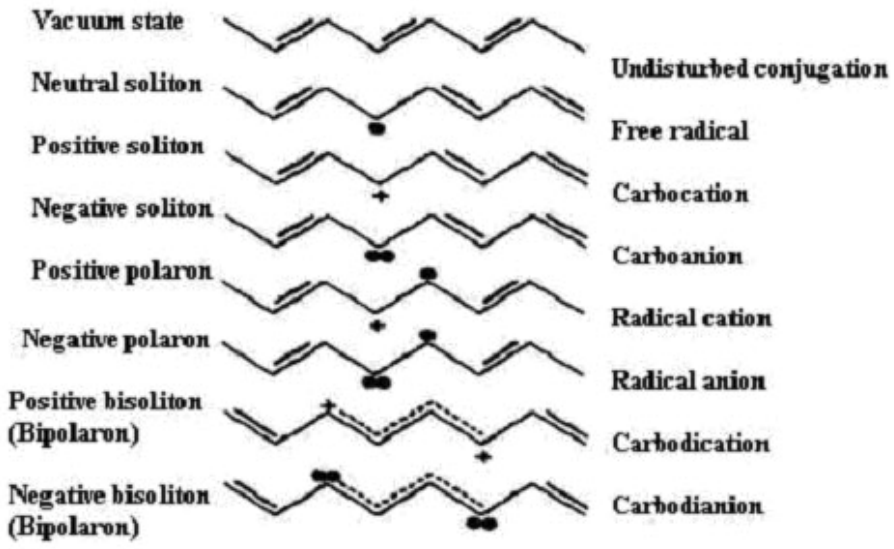

Figure 1.6 Defects created in conjugated chains

Doping is a reversible process with little or no degradation of the polymer backbone. Both doping and undoping processes, involving dopant counterions which stabilize the doped state, may be carried out chemically and electrochemically [9]. Photo-doping and charge-injection doping, which introduce no dopant ions are also known [10].

The p-doping, i.e. partial oxidation of the π-backbone of an organic polymer, was first discovered by treating *trans*-$(CH)_x$ with an oxidizing agent such as iodine [3,8]:

$$trans\text{-}\left[CH\right]_x + 1.5\ xyI_2 \longrightarrow \left[CH^{y+}(I_3)_y^-\right]_x \tag{1.1}$$

The p-doping can also be accomplished by electrochemical anodic oxidation by immersing a *trans*-$(CH)_x$ film in, e.g. a solution of $LiClO_4$ and attaching it to the positive terminal of a dc power source, the negative terminal being attached to an electrode also immersed in the solution [11]:

$$trans\text{-}\left[CH\right]_x + xy(ClO_4)^- \longrightarrow \left[CH^{y+}(ClO4)_y^-\right]_x + (xy)e^- \tag{1.2}$$

The n-doping, i.e. partial reduction of the backbone π-system of an organic polymer, was also discovered using *trans*-$(CH)_x$ by treating it with a reducing agent such as liquid sodium amalgam or preferably sodium naphthalide [3,8]:

$$trans\text{-}\left[CH\right]_x + (xy)Na^+(Nphth)^- \longrightarrow \left[Na_y^+(CH)^{-y}\right]_x + Nphth \tag{1.3}$$

The n-doping can also be carried out by electrochemical cathodic reduction by immersing a *trans*-$(CH)_x$ film in, e.g. a solution of $LiClO_4$ and attaching it to the negative terminal of a dc power source, the positive terminal being attached to an electrode also immersed in the solution [12]:

$$trans\text{-}\left[CH\right]_x + xyLi^+ + (xy)e^- \longrightarrow \left[Li_y^+(CH)^{-y}\right]_x \tag{1.4}$$

To sum up, doping agents or dopants are either strong reducing or oxidizing agents. They may be neutral molecules and compounds or inorganic salts, which can easily form ions, organic dopants or polymeric dopants and the nature of dopants, play an important role in the stability of conducting

polymers [13]. In Figure 1.8 conductivities of some conducting polymers with selected dopants are displayed.

1.2.2.2 Hopping

The conduction process is described with two important mechanisms, doping and hopping. Hopping is simply intra-chain, inter-chain and inter-particle motion of charges in a polymer matrix. The intra-chain movement, motion of the charge carrier through a single chain, depends on the efficient conjugation. On the other hand, the inter-chain movement, jumping from one chain to another, is determined by the piling of the polymer chains. The mobility also depends on the movement of electrical charges from particle to particle. To sum up, the mobility and therefore conductivity are determined on both a macroscopic (inter-particle) and microscopic (intra- and inter-chain) level.

1.3 Synthesis of Conducting Polymers

Conducting polymers may be synthesized by any one of the following techniques [13]:

1. Chemical polymerization
2. Electrochemical polymerization
3. Photochemical polymerization
4. Metathesis polymerization
5. Concentrated emulsion polymerization
6. Inclusion polymerization
7. Solid-state polymerization
8. Plasma polymerization
9. Pyrolysis
10. Soluble precursor polymer preparation

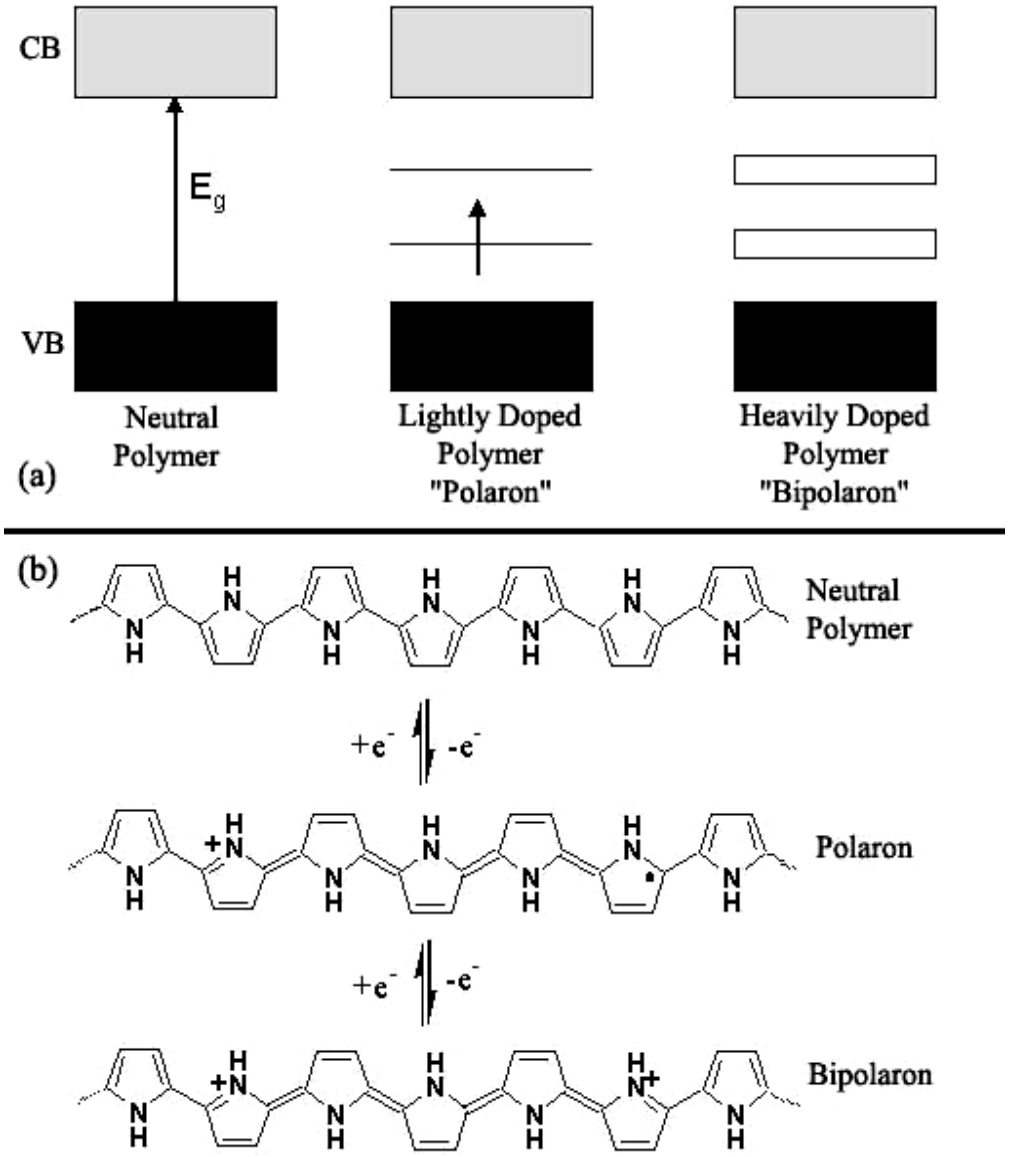

Figure 1.7 Band theory and doping-induced structural transitions of polypyrrole: (a) Band theory of conjugated polymers (b) Structural changes associated with polaron and bipolaron formation as a result of oxidative doping in polypyrrole

Polymer	Structure	Doping materials	$\Omega^{-1}cm^{-1}$
Polyacetylene	(CH)n	I_2, Br_2, Li, Na, AsF_5	10000
Polypyrrole	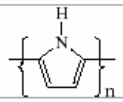	BF_4^-, ClO_4^-	500-7500
Polythiophene	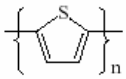	BF_4^-, ClO_4^-	1000
Poly(3-alkylthiophene)	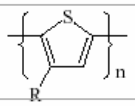	BF_4^-, ClO_4^-	1000-10000
Polyphenylene sulfide	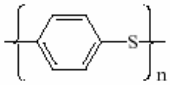	AsF_5	500
Polyphenylenevinylene	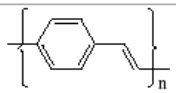	AsF_5	10000
Polythienylenevinylene	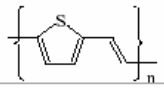	AsF_5	2700
Polyphenylene	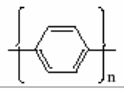	AsF_5, Li, Na	1000
Polyisothianaphthene	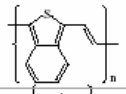	BF_4^-, ClO_4^-	50
Polyazulene	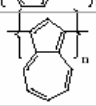	BF_4^-, ClO_4^-	1
Polyfuran	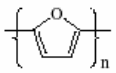	BF_4^-, ClO_4^-	100
Polyaniline	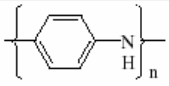	HCl	200

Figure 1.8 Conductivities of some conducting polymers with selected dopants

1.3.1 Chemical Polymerization

Chemical polymerization is useful when large amounts of conducting polymer needed. In chemical polymerization relatively strong chemical oxidants such as ammonium peroxidisulfate (APS), ferric ions, permanganate or bichromate anions, or hydrogen peroxide are utilized. These oxidants are able to oxidize the monomers in appropriate solution, leading to chemically active cation radicals of the monomers used. The cation radicals formed upon attack of the oxidants react with monomer molecules, yielding oligomers and then polymers. Chemical polymerization occurs in the bulk of the solution, and the resulting polymers precipitate as insoluble solids. However, a part of conducting polymer can deposit spontaneously on the surface of various materials, immersed into the polymerization solution [14]. In the eq.1.5 oxidative polymerization with $FeCl_3$ of a five membered heterocyclic compound is shown [15].

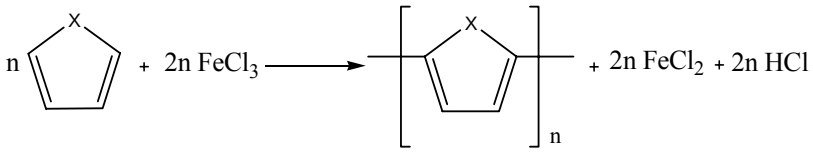

(1.5)

1.3.2 Electrochemical Synthesis

Electrochemical polymerization is a convenient technique when a polymer film with controlled thickness is required. Electrochemical oxidation of numerous resonance stabilized aromatic molecules, such as pyrrole, thiophene, aniline, furan etc., produces electronically conducting polymers. The polymerization is believed to involve either radical-cation/radical cation coupling or reaction of a radical cation with a neutral monomer (Figure 1.9) [16,80]. The mechanism of electropolymerization of the five membered heterocycle, with radical-cation/radical-cation coupling and resonance

stabilization after removal of an electron are shown in Figures 1.10 and 1.11, respectively.

After the loss of two protons and re-aromatization, a dimer forms. The dimer (and succeeding oligomers) is more easily oxidized than the monomer and the resulting dimer radical cation undergoes further coupling reactions, proton loss and re-aromatization. Electropolymerization proceeds through successive electrochemical and chemical steps according to a general E(CE)n (E for electrochemical, C for chemical) scheme, until the oligomers become insoluble in the electrolyte solution and precipitate onto the electrode surface [17].

Since conjugated oligomers are oxidized at less positive potentials than their corresponding monomer, polymer oxidation occurs concurrently with electro-deposition.

In the oxidized state, conducting polymers are p-doped and have delocalized π-band structure; the charge on the chain is balanced with counter anions. Upon reduction, counter anion exits or cation of the electrolyte enters, electronic conjugation is removed and polymer is in insulating regime (Figure 1.12). Typically, one electron is removed from the polymeric backbone for every three-four monomer units to form polar structures, responsible for inherent conductivity.

It is generally believed that oxidative coupling occurs at sites on the heterocyclic ring where a high spin density resides for the radical cation. For thiophene, pyrrole, and furan, the highest spin densities have been measured at the 2- and 5-positions, also referred to as the α positions [18,19]. The 3- and 4-positions (referred to as the β positions) have also measurable spin densities, therefore some coupling reactions may occur at these positions. Various coupling events for the electrochemical polymerization of pyrrole are shown in Figure 1.13. However, α-β and β-β coupling generally result in irregular backbones and poor electronic properties in conducting polymers. “Blocking” the 3- and 4-positions of the monomer by the attachment of various alkyl and alkoxy groups can eliminate these chain imperfections discussed. In addition,

several other electronic properties are noticeably affected by the structural modifications including monomer oxidation potential, electronic band gap, and electrochromic properties of the resultant polymers.

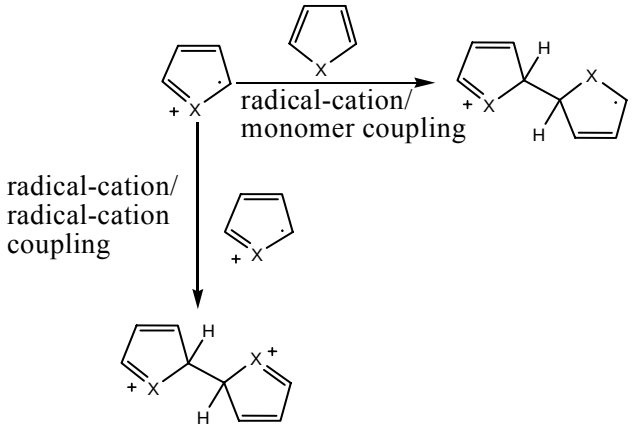

Figure 1.9 Radical-cation/monomer and radical-cation/radical cation coupling where X = N-H, S, O

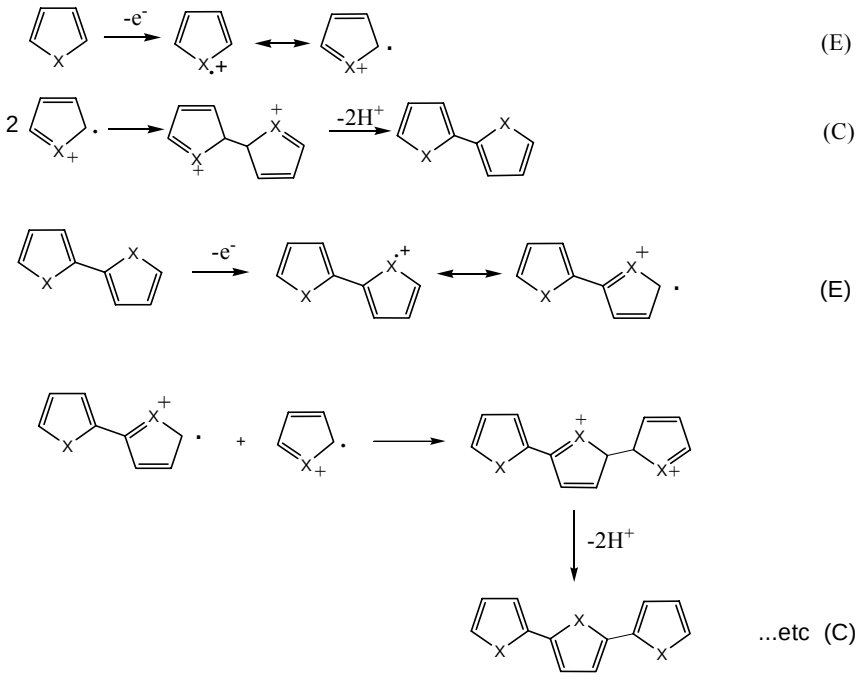

Figure 1.10 Proposed mechanism for electropolymerization of a five membered heterocyclic compound, where X = N-H, S, O

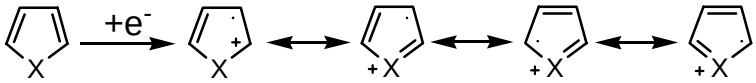

Figure 1.11 Resonance stabilization of a five membered heterocyclic compound upon formation of radical-cation where X = N-H, S, O

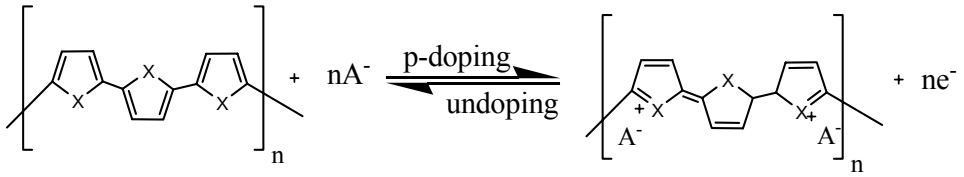

Figure 1.12 Undoping, p-doping in a conducting polymer

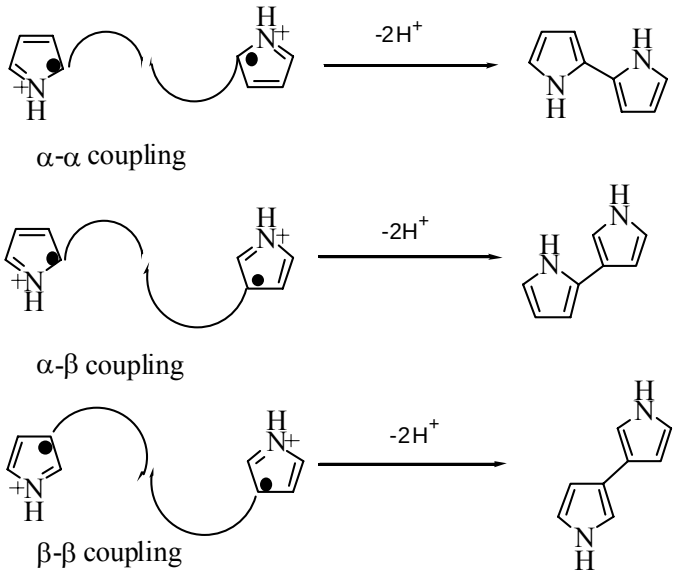

Figure 1.13 Coupling reactions for pyrrole during oxidative polymerization.

Electrochemical polymerization has some advantages over chemical polymerization:

✓ Simple

- ✓ Selective
- ✓ Reproducible
- ✓ Reactions are done at room temperature
- ✓ Thickness of the films can be controlled
- ✓ It is possible to produce homogenous polymers
- ✓ Doping of the polymer can be achieved with the desired ion simultaneously
- ✓ The molecular weight distributions can be controlled
- ✓ Films are directly formed at the electrode surface
- ✓ Graft and block copolymers can be easily obtained

Monomers used in electrochemical polymerization are aromatic and can be oxidized at relatively low anodic potentials. This removes the complications arising from the oxidative decomposition of the solvent and supporting electrolyte.

Since the polymerization involves radical cation intermediates, nucleophilicty of the reaction medium plays an important role. For this reason, experiments are performed in aprotic solvents with completely dissociated supporting electrolytes in them. In addition, since an oxidative process produces films, it is important that electrodes utilized do not oxidize concurrently with the monomer. That's why; mostly platinum or gold electrodes are employed.

1.3.3 Electrochemical Polymerization in Lewis Acid

Boron fluoride-ethyl ether (BFEE) is utilized to lower the oxidation potential of some heterocyclics like thiophene, pyrrole and bithiophene. Electrochemical polymerization of thiophene in BFEE yields a free standing film with good quality mechanical properties [20]. High potentials applied may cause the degradation of the polymer as well as side reactions of the electrolytes and electrodes [21]. In BFEE, aromaticity of thiophene is somewhat reduced by the interaction with Lewis acid. Increasing the acidity

of Lewis acid solution results in a decrease in the aromaticity of the thiophene ring and lowers the oxidation potential of the monomer [22].

1.3.4 Electrochemical Synthesis of Conducting Copolymers

Conducting polymers are very promising materials thanks to their conductivities, stability against environmental conditions and ease in preparation. However, they have poor mechanical properties; they are insoluble, non-melting, and thus not processible. Various methods such as the grafting alkyl groups into the main chain, the synthesis of soluble precursors and preparation of conducting polymer composites, blends and copolymers can be used to improve mechanical properties [23]. Copolymers from pyrrole, pyrrole derivatives, thiophene, bithiophene and other combination of aromatic compounds have been reported [24-28].

Common approach for the preparation of conducting copolymers is electropolymerization of the conducting component on electrode previously coated with the insulating polymer. In these cases, comonomer, solvent molecules and electrolyte anions swell the polymer film as they diffuse into the polymer coating. Polymerization starts in the interface between the electrode surface and the insulating polymer film, at the end a conducting copolymer film is obtained. Electrochemical polymerization of pyrrole and thiophene may occur on an ordinary insulating polymer film [29-31]. In addition, by dissolving the monomer and the comonomer in the same solvent and applying an appropriate potential, conducting copolymer may be obtained onto the electrode surface.

Polycarbonate and polystyrene [32], poly (methyl methacrylate) [33-35], polyimide [36], polyamide [37], polysiloxanes [38], poly (tetrahydrofuran) [39, 40] were previously used as the host matrices.

1.4 Characterization of Conducting Polymers

Conducting polymers can be characterized by various analytical techniques. Many examples exist in the literature, some of which include; cyclic voltammetry for understanding reduction-oxidation behavior of conducting polymers, optoelectronic characterization for examination of π to π^* transitions, nuclear magnetic resonance and FTIR for structure confirmation, gel permeation chromatography for molecular weight, differential scanning calorimetry and thermogravimetry analysis for evidence of glass and melting transitions and decomposition temperatures.

1.5 Application of Conducting Polymers

Conducting polymers were initially attractive because of the fundamental interest in them and the doping induced metal-insulator transition. However, the chemistry and physics of these polymers in their non-doped semiconducting state are of great interest because they provide a route to 'plastic electronic' devices [6]. To illustrate, upon electrochemically doping and undoping, change in color is observed for conducting polymers, thus they are widely utilized in electrochromic devices (ECDs) or 'smart windows' [41-46]. In addition, conducting polymers are used in organic light emitting diodes (OLEDs) [47-49] enzyme immobilization [50-52], gas sensors [53, 54], solar cells [55, 56], EMI shielding [57], field effect transistors [FETs] [58] and polymer batteries [59].

1.6 Electrochromism

Electrochromism can be defined as the persistent change of optical properties of a material induced by reversible redox process [60]. Electrochromic devices or displays (ECDs) have potential use in various applications. To illustrate, ECDs may be used in automotive industry as rear-

view windows and in architecture as smart windows to control luminosity as well as saving energy.

1.6.1 Types of Electrochromic Materials

There are three main types of electrochromic materials. First group of electrochromic materials are soluble in the electrolysis solution at both redox states, the second type materials are soluble in either reduced or oxidized state and a thin film forms on the electrode surface following electron transfer, the last group including conducting polymers has both solid redox states and they are studied in thin solid forms on the electrodes [16].

1.6.2 Chemical Classes of Electrochromic Materials

There is a vast number of chemical species possessing electrochromic properties. Viologens [61], transition metal oxides, most famously tungsten trioxide (WO_3) systems [62-64], prussian blue systems [65], phthalocyanines [66, 67], and conducting polymers [68] are widely utilized electrochromic materials.

1.6.3 Conducting Polymers as Electrochromic Materials

All conducting polymers are potentially electrochromic, the doping process modifies their electronic structure, producing new electronic states in the band gap and causing the color changes [60] (Figure 1.14). Upon doping optical absorption shifts towards the higher wavelengths, i.e. lower energy part of the spectrum. The color change or optical contrast between redox states depends on the band gap energy of the polymer. Thin films of conducting polymers with Eg greater than 3 eV (~400 nm) are colorless and transparent in the reduced form, upon doping they absorb in the visible region. Those with Eg equal to or less than 1.5 eV (~800 nm) are highly absorbing in the reduced

form but, after oxidizing or doping the absorption is relatively weak in the visible region as it is transferred to the near infrared. Polymers with intermediate gaps have distinct optical changes throughout the visible region and can be made to induce many color changes [16].

If the band gap energy is reduced the population in the conductance band will be increased, thus real 'synthetic metals' will be produced. Reduction of the band gap is associated also with low oxidation potential of the polymeric material. The most usual way to modify the HOMO and LUMO levels of a conjugated system involves introducing electron donating or withdrawing substituents that will respectively increase the HOMO level or lower the LUMO level [69].

Polythiophenes [17] are widely used as electrochromic materials due to their ease in the synthesis, and environmental stability. The parent polymer, polythiophene that is abbreviated as PTh, has red color in the reduced state and after oxidation its color changes to blue. Another class of organic electrochromic materials is polypyrroles (PPys). PPy has lower oxidation potential than PTh and its color alters between yellow, red and blue upon undoping and doping. Polyaniline films are multielectrochromic and yellow-green-blue-black colors are observed [70].

1.7 Experimental Methods for Studying Electrochromic Polymers

Conducting polymers which are electroactive are usually potentiostatically coated onto working electrode and three-electrode circuitry is utilized for this purpose. Working electrode substrates are generally made of glass or a flexible plastic, e.g. poly(ethylene terephthalate) (PET), sheet coated with an optically transparent electrically conducting film, e.g. tin doped indium oxide (ITO), antimony doped tin oxide, or fluorine-doped tin oxide [16]. After the material is deposited onto the substrate, it is placed in a monomer free electrolyte, and spectroelectrochemistry, optical contrast, switching speed and colorimetry of the material are investigated.

Electrochromic device (ECD) is simply an electrochemical cell assembled of two electrodes, primary electrochromic electrode and a charge balancing secondary electrode, and a gel electrolyte [16]. In dual type ECDs, both of the electrodes are coated with electrochromic materials, one electrochromic material is colored when oxidized (anodic coloration) and the other is colored when reduced (cathodic coloration).

The requirements for high performance electrochromic devices are [60]:

- High electrochromic efficiency, expressed in $cm^2\ C^{-1}$ and related to the injected charge in the material to change its color;
- Short electronic response time;
- Good stability;
- Optical memory, defined as the color stability under open circuit potential conditions;
- Optical contrast, also called write-erase efficiency
- Color uniformity.

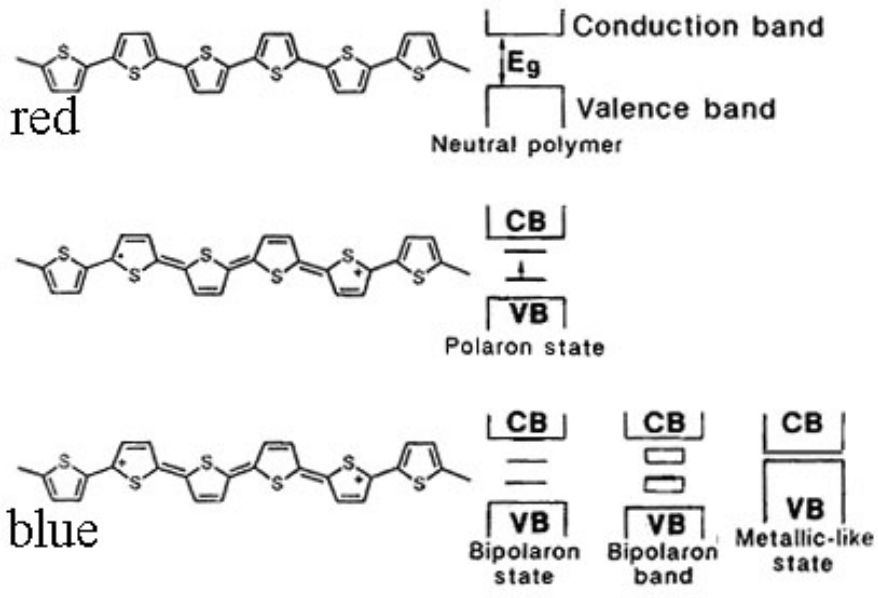

Figure 1.14 Evolution of electronic band structure with p-doping for conjugated polymer with non-degenerate ground state.

1.7.1 Spectroelectrochemistry

In their neutral state, conducting polymers are in insulating regime with a band gap, Eg, between the valence band (HOMO) and the conduction band (LUMO). Upon oxidizing or doping, the band structure of the polymer is modified, in other words lower energy intraband transitions occurred as well as charged carriers (polarons and bipolarons) are created, as a consequence the conductivity is increased. Spectroelectrochemistry is crucially important in determination of π to π^*, polaronic and bipolaronic transitions in addition to calculation of band gap energy.

1.7.2 Optical Contrast and Switching Speed

Optical contrast is an essential parameter to evaluate an electrochromic material. It is frequently reported as percent transmittance change (Δ%T) between the two colored redox states at a specific wavelength where the highest contrast is monitored. Switching speed is the time required for the coloring/bleaching process of an electrochromic material. The switching speed of electrochromic material is dependent on ionic conductivity of the electrolyte, ion diffusion in thin films, magnitude of the applied potential, film thickness and morphology of the film [71].

1.7.3 Colorimetry

The colorimetry analysis is based on a mathematical representation of a color on CIE (Commission Internationale de l'Eclairage) Yxy or L a b color space. Y coordinate represents brightness or luminance of a color whereas xy coordinate defines hue and saturation. After the color of the material is measured with a colorimeter on Yxy coordinates, throughout a computer program Yxy values can be transformed to its L a b reciprocals. Colorimetry is an effective and objective method to define a color giving accurate plus

precise description of color. In L a b system, L, a and b stand for luminance, hue and saturation, respectively. Luminance is simply transmittance of light through a sample as perceived by human eye, hue is commonly referred as color and represents dominant wavelength, and saturation defines intensity or purity of a certain color. Figure 1.15 shows the color space of the CIE.

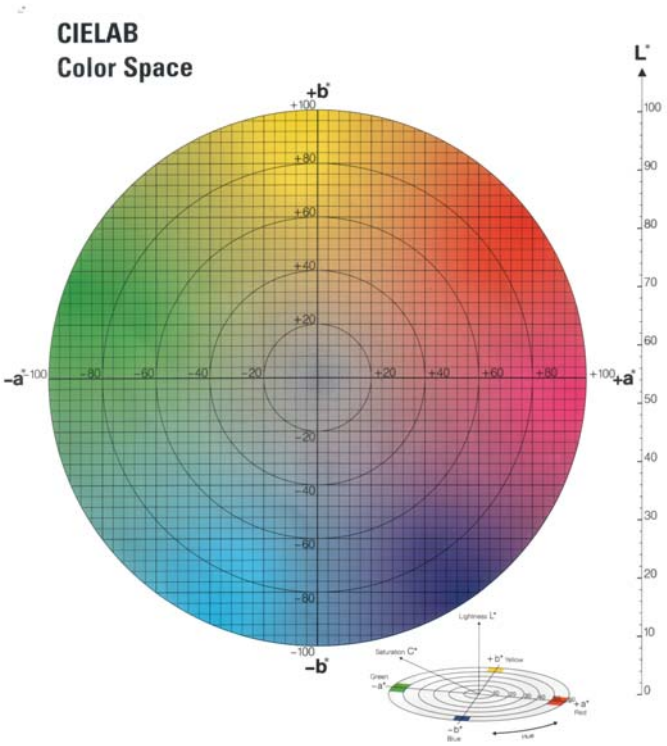

Figure 1.15 CIE L a b color space

1.7.4 Optical Memory and Stability

Optical memory or open-circuit memory is defined as the time the material retains its absorption state after the electric field is removed. Electrochemical stability or shortly said stability experiments measure the degradation period of the active redox couple since after some cycling performance of the material is decimated [71].

1.8 Aims of the Work

Aims of the work are: To synthesize two different thiophene functionalized monomers, which are named as terephthalic acid bis-(thiophen-3-ylmethyl)thioester (TTMT) and fully conjugated 1-(4-fluorophenyl)-2,5-di(thiophen-2-yl)-1*H*-pyrrole (FPTP); electrochemically polymerize or copolymerize them with other well known comonomers in thin film forms; after that examine the electrochromic properties of the homopolymers plus copolymers, construct electrochromic devices with PEDOT and finally evaluate the electrochromic performances of these devices.

CHAPTER II

EXPERIMENTAL

2.1 Materials

3-Methylthiophene (Aldrich), N-Bromosuccinimide (NBS) (Fluka), benzoyl peroxide (Sigma), carbon tetrachloride (Riedel-de Haen), thiourea (Sigma), methanol (Merck), sodium hydroxide (Aldrich), sulfuric acid (Merck), benzene (Merck), magnesium sulphate (Aldrich), triethylamine (TEA) (Aldrich), dichloromethane (Merck), terephthaloyl dichloride (Acros), hydrochloric acid (Merck), distilled water, sodium sulphate (Aldrich), ethanol (Merck) were used as received in the synthesis of terephthalic acid bis-(thiophen-3-ylmethyl)thioester. Acetonitrile (AN) (Merck), boron trifluoride diethyl etherate (BFEE) (Aldrich), tetrabutylammonium terafluoroborate (TBAFB) (Aldrich) were used without purification in the electrochemical copolymerization of TTMT with thiophene and pyrrole. Thiophene (Th) and pyrrole (Py) were both purchased from Aldrich and distilled before use. 3, 4-Ethylenedioxythiophene (EDOT) (Aldrich) was used with no further purification. The gel electrolyte was prepared by blending polymethylmethacrylate (PMMA) (Aldrich), TBAFB, acetonitrile, and propylene carbonate (PC) (Aldrich).

Aluminium chloride ($AlCl_3$) (Aldrich), dichloromethane, succinyl chloride (Aldrich), hydrochloric acid, sodium hydrogencarbonate ($NaHCO_3$) (Aldrich), magnesium sulphate, 4-fluoroaniline (Aldrich), propionic acid

(Aldrich), toluene (Sigma) were used as received in the synthesis of 1-(4-fluorophenyl)-2,5-di(thiophen-2-yl)-1*H*-pyrrole (FPTP). Thiophene (Th) was distilled before use. Nitromethane (Aldrich), iron(III)chloride hexahydrate ($FeCl_3.6H_2O$) (Aldrich), chloroform (Merck), and methanol were utilized in chemical polymerization, whereas AN, lithium perchlorate ($LiClO_4$) (Aldrich) and sodium perchlorate ($NaClO_4$) (AnalaR) were used in electrochemical polymerization as obtained. The gel electrolyte was prepared by blending PMMA, $LiClO_4$, $NaClO_4$, AN, and PC.

2.2 Equipment

2.2.1 Nuclear Magnetic Resonance (NMR) Spectrometer

^{1}H-NMR and ^{13}C-NMR spectra of the monomers and the chemical polymer of FPTP were recorded on a Bruker-Instrument-NMR Spectrometer (DPX-400) with $CDCl_3$ as the solvent and chemical shifts (δ) were given relative to tetramethylsilane as the internal standard.

2.2.2 Fourier Transform Infrared (FTIR) Spectrometer

FTIR spectra of the samples were recorded on a Nicolet 510 FTIR spectrometer for the detection of functional groups. Samples were prepared as KBr pellets.

2.2.3 Cyclic Voltammetry (CV) System

Cyclic voltammetry is a convenient technique to determine the oxidation-reduction peak potentials of the monomers and the electroactivity of polymers.

The CV system was composed of a potentiostat, a function generator, an XY recorder, and a cyclic voltammetry cell. Function generator or wave generator applies a triangular wave potential to the cell so that the working

electrode potential is swept linearly through the voltammetry wave (Figure 2.1). During these scans, potential-time response and current (I) versus potential (V) curves are obtained.

A typical cyclic voltammogram recorded for a reversible single electrode transfer reaction is shown in Figure 2.2. Solution contains only a single electrochemical reactant. The forward scan produces a current peak for any analytes that can be reduced through the range of the potential scan. The current will increase as the potential reaches the reduction potential of the analyte, but then falls off as the concentration of the analyte is depleted close to the electrode surface. As the applied potential is reversed, it will reach a potential that will reoxidize the product formed in the first reduction reaction, and produce a current of reverse polarity from the forward scan. This oxidation peak will usually have a similar shape to the reduction peak. The peak current, i_p, is described by the Randles-Sevcik equation:

$$i_p=(2.69*10^5)\, n^{3/2}\, A\, C\, D^{1/2}\, v^{1/2} \qquad (2.1)$$

where n is the number of moles of electrons transferred in the reaction, A is the area of the electrode, C is the analyte concentration (in moles/cm^3), D is the diffusion coefficient, and v is the scan rate of the applied potential.

Cyclic voltammetry experiments were carried out at room temperature and under nitrogen atmosphere in a three electrode cell (Figure 2.3) consisting of platinum (Pt) wire as the counter, silver (Ag) wire as the reference, ITO (indium doped tin oxide) coated glass as the working electrode. AN was utilized as solvent in all experiments whereas BFEE was used to lower the oxidation-reduction potentials in the experiments carried out with TTMT in the presence of Th. TBAFB (0.1 M) and $LiClO_4$ (0.1 M) /$NaClO_4$ (0.1 M) salts were used as supporting electrolytes. Bank Wenking POS 2 and Solatron 1285 potentiostat/galvanostat were utilized for electrochemical studies.

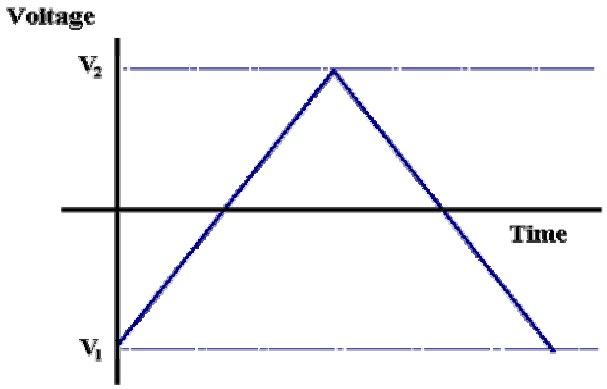

Figure 2.1 Triangular wave function

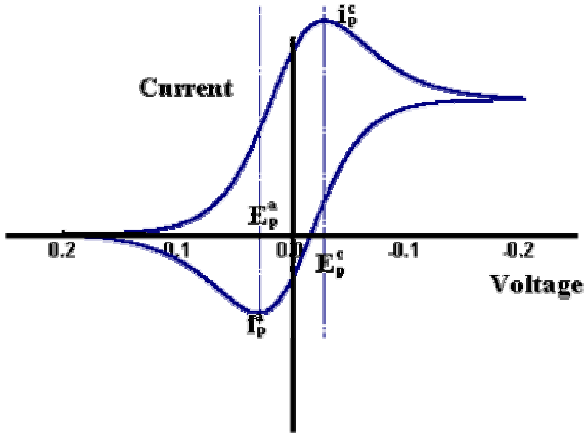

Figure 2.2 A cyclic voltammogram for a reversible redox reaction

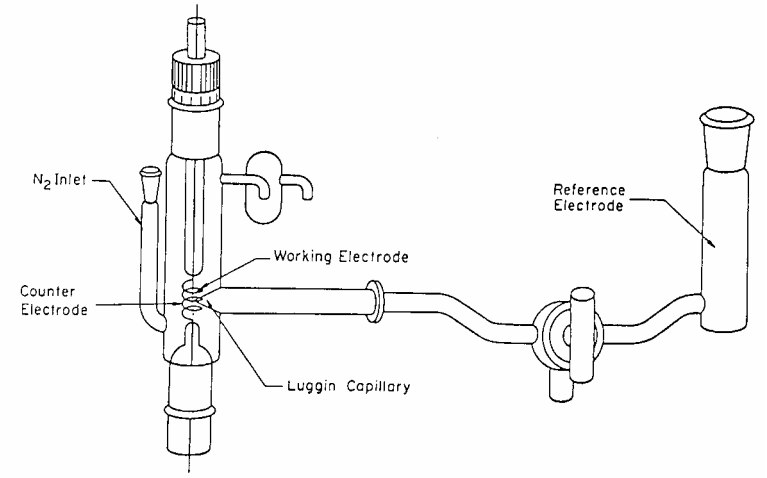

Figure 2.3 Cyclic voltammetry cell

2.2.4 Electrolysis Cell

In the electrochemical synthesis of conducting polymers constant potential (potentiostatic) electrolysis or constant current (galvanostatic) electrolysis are used.

Constant current electrolysis (CCE) is carried out in a single compartment cell equipped with two Pt electrodes, which are working and counter electrodes. The current is controlled during the electrolysis and the potential is allowed to change. The film thickness can be easily controlled by inspection of the polymerization time. Variation of applied potential may lead to some side reactions.

Constant potential electrolysis (CPE) is performed in a dual compartment cell furnished with three electrodes: Pt working, Pt counter, Ag wire capillary reference electrodes (Figure 2.4). The total volume of the electrolysis cell utilized was 50 mL. The cell has gas inlets, if inert atmosphere is needed N_2 gas may be bubbled through them. The compartments of working and counter electrodes were separated with a porous sintered glass in order to prevent possible side reactions. The voltage difference between the reference and the working electrodes is called as the polymerization potential.

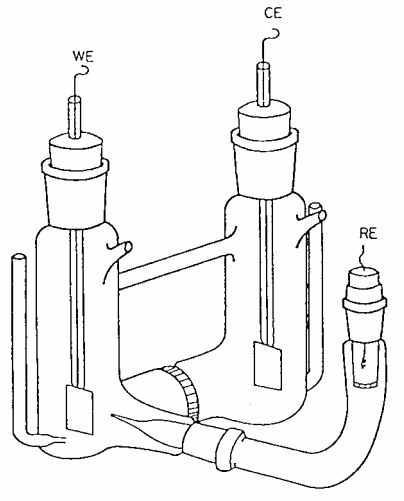

Figure 2.4 Constant potential electrolysis cell

2.2.5 Potentiostat

Potentiostat, used in constant potential electrolysis, keeps the voltage difference between working electrode and reference electrode at a constant value despite the changes in the current passing through the electrolytic cell.

During the electrolysis Wenking Pos 73 potentiostat was utilized to supply the polymerization potential. For the electrochromic properties of the polymers, Solatron 1285 and Volta Lab® PST050 potentiostats were used.

2.2.6 Thermal Analysis

Melting points of the monomers were determined with Schmelzpunktgeräte SMP II. Thermal behaviors of the polymers synthesized were examined by means of differential scanning calorimeter (DSC) named as Du Pont 2000. The differential calorimetry (DSC) experiments were carried out under N_2 atmosphere and the heating rate was 10 °C/min.

2.2.7 Scanning Electron Microscopy (SEM)

Surface morphologies of the polymer films were examined with JEOLJSM-6400.

2.2.8 Gel Permeation Chromatography (GPC)

Mn and Mw of the polymer obtained by chemical polymerization were determined with PL-220 gel permeation chromatography.

2.2.9 Four Probe Conductivity Measurements

Among available conductivity measurement techniques, four-probe method gives more accurate results in determination of electrical properties of

conducting polymers. This technique eliminates errors caused by contact resistance, since the two contacts measuring the voltage drop are different from the contacts applying the current across the sample.

Figure 2.5 shows the simplest form of a four-probe measurement setup. A row of pointed electrodes touches the surface of a polymer film taped or spin cast on an insulating substrate. A known current (I) is injected at the electrode 1 and is collected at the electrode 4, while the potential difference ΔV between contacts 2 and 3 is measured. Conductivity is calculated from the following equation:

$$\sigma = \ln 2 / (\pi R t) \qquad (2.2)$$

where R is the resistance of the sample, and t is the thickness.

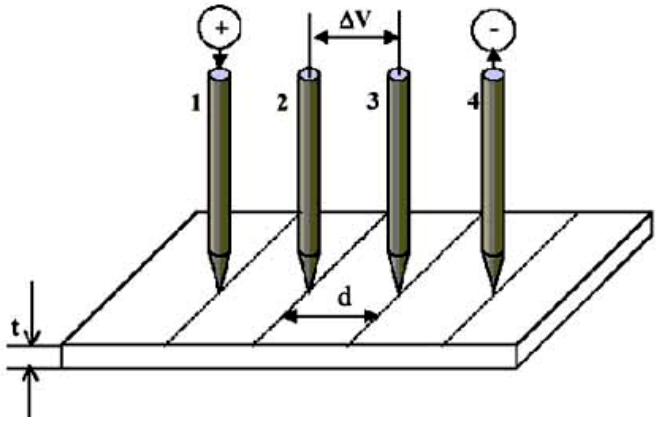

Figure 2.5 Four probe conductivity measurement

2.2.10 Spectroelectrochemistry Experiments

Spectroelectrochemical and kinetic studies were performed on Solatron 1285 potentiostat/galvanostat attenuated with Agilent HP8453A UV-Vis spectrophotometer in addition to VoltaLab® PST050 potentiostat coupled with Varian Cary 5000 UV-Vis-NIR spectrophotometer in a cell furnished

with ITO coated glass working, Pt wire counter electrodes and a Ag/Ag^{+} reference electrode at room temperature.

2.2.11 Colorimetry Measurements

For colorimetry measurements Conica Minolta CS-100 A chromameter was used.

2.3 Procedure

2.3.1 Synthesis of Terephthalic Acid Bis-(thiophen-3-ylmethyl)Thioester (TTMT)

3-Methylthiophene was brominated with the use of NBS [72] and the resultant product, 3-bromomethylthiophene, was converted to thiophen-3-yl methanthiol via the synthesis route proposed by Denise and Paul Cagniant [73]. To obtain 3-bromomethylthiophene, 3-methylthiophene (10 mL, 0.100 mol), NBS (18 g, 0.100 mol) were refluxed for 6 h in 30 mL carbon tetrachloride containing 0.08 g (0.003 mol) of benzoyl peroxide. After cooling in an ice-bath, the by-product NBS was removed by filtration, the reaction medium was washed with carbon tetrachloride and the solvent was evaporated. The remaining oily substance was distilled in vacuum and 5.13 g (0.028 mol) of 3-bromomethylthiophene was obtained. The product was immediately refluxed with equimolar thiourea for 2 h in 30 mL of methanol. The expected product was crystallized in this solution after leaving for 24 h in cold. 6.2 g (0.025 mol) of isothiouronium salt were obtained. The resulting salt was dissolved in 30 mL of methanol and refluxed for 2 h with 0.049 mol of sodium hydroxide. Methanol was evaporated and the medium was acidified until pH 7.00. After extracting with benzene, water present in the organic layer was trapped with magnesium sulphate. Subsequent to filtering magnesium sulphate and evaporating benzene, thiophen-3-ylmethanethiol

synthesis was completed and 2.11 g (0.016 mol) of substance were obtained. Thiophen-3-ylmethanethiol was dissolved in 15 mL of triethylamine and 30 mL of dichloromethane. 1.62 g (0.008 mol) of terephthaloyl dichloride was dissolved in 30 mL of dichloromethane and added dropwise to the first solution with continuous stirring. The final reaction was carried out for 24 h in an ice-bath and under nitrogen atmosphere. The resulting substance was washed with 1% hydrochloric acid solution and with water. Extraction was done with dichloromethane, the organic layer was dried over sodium sulphate, and then filtered; the solvent was removed via rotaevaporatory. The target material, terephthalic acid bis-(thiophen-3-ylmethyl)thioester (TTMT) (0.32 g, 0.001 mol) was obtained by twice recrystallization in ethanol. The synthesis route is shown in Figures 2.6 a and b.

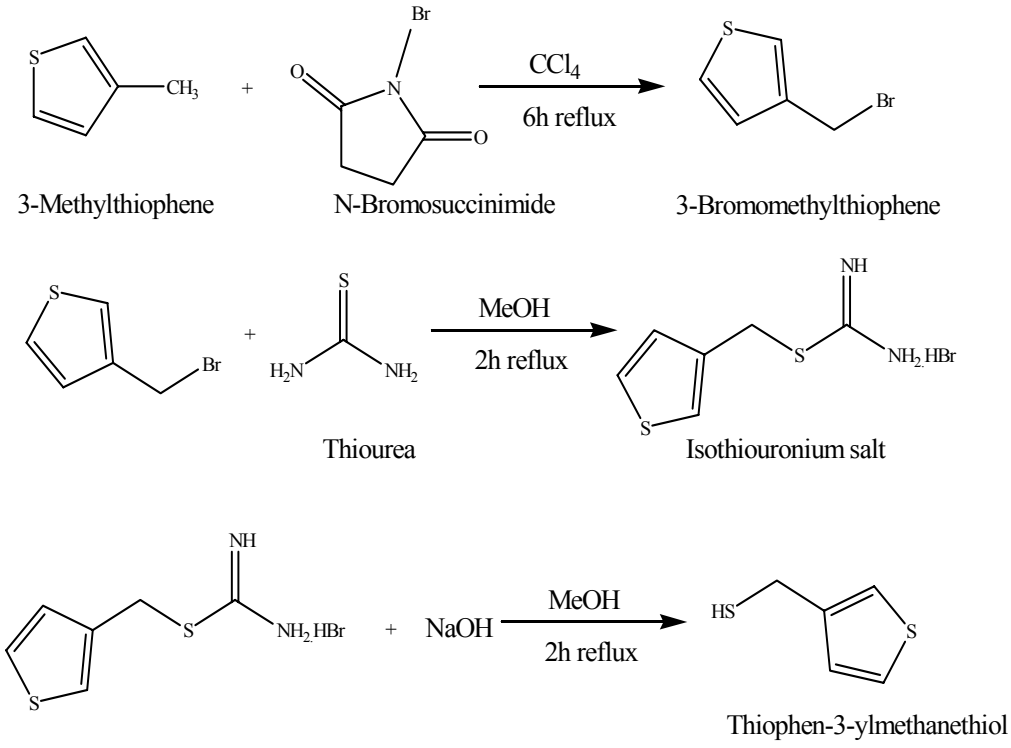

Figure 2.6 a Synthesis route of thiophen-3-ylmethanethiol

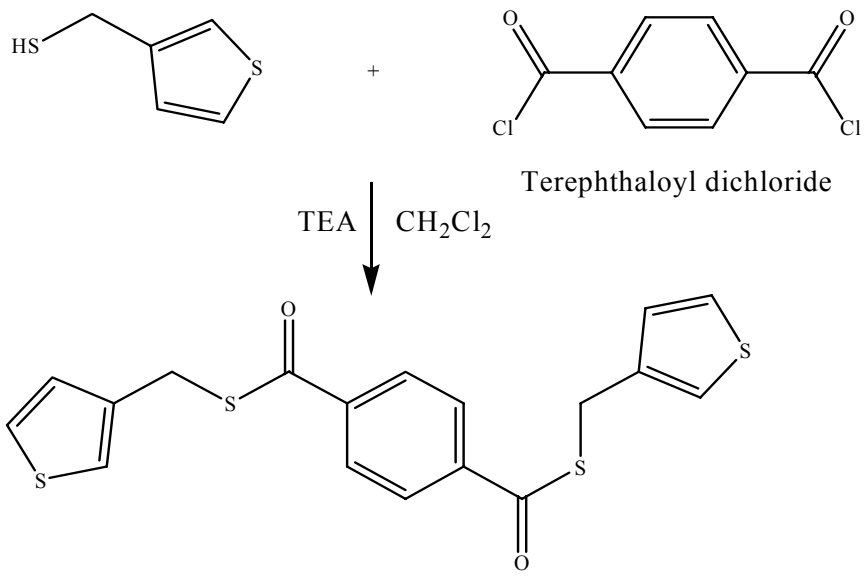

Figure 2.6 b Synthesis route of TTMT

2.3.2 Synthesis of 1-(4-fluorophenyl)-2,5-di(thiophen-2-yl)-1*H*-Pyrrole (FPTP)

Two main routes were commonly used in order to synthesize the monomer 1-(4-fluorophenyl)-2,5-di(thiophen-2-yl)-1*H*-pyrrole (FPTP), as shown in Figure 2.7. The first one was based on the synthesis of 1,4-di (2-thienyl)-butane-1,4-dione and the second one, Knorr-Paal reaction, was the dehydrative cyclization of diketone with an amine.

1,4-di(2-thienyl)-butane-1,4-dione was synthesized by the method proposed in the literature [74-75]. It was prepared by Friedel-Crafts acylation of thiophene with succinyl chloride. To a suspension containing 8.1 g (0.06 mol) of $AlCl_3$ in 30 mL of dichloromethane, a solution of thiophene (4.8 mL, 0.06 mol) and succinyl chloride (2.75 mL, 0.025 mol) in 30 mL of dichloromethane were added dropwise at 18-20°C, and the mixture was stirred for 4 h at that temperature. The suspension was poured into a mixture of 50 g ice and 5 mL hydrochloric acid and further stirred for 30 min. The organic

layer was separated and the aqueous layer was extracted with dichloromethane. The organic layer and the extract were combined and washed with water and aqueous $NaHCO_3$, dried over $MgSO_4$, separated by column chromatography on silica gel (eluent: dichloromethane), and crude product was recrystallized from chloroform-hexane.

1-(4-Fluoro-phenyl)-2,5-di(2-thienyl)-1*H*-pyrrole (FPTP) has previously been synthesized by the same method in literature [76-77] from dehydrative cyclization of diketone with an amine. 1.25 g (5 mmol) of the 1,4-di (2-thienyl)-butane-1,4-dione (DTBD), 0.66 mL (7 mmol) of the 4-fluoraniline, 0.45 mL (5.4 mmol) of propionic acid were dissolved in 25 mL of toluene. The mixture was stirred and refluxed for 24 h under argon atmosphere. Toluene was evaporated and the product was separated by column chromatography on silica gel (eluent: dichloromethane). The desired compound (1g, 65%) was obtained from elution at the solvent front.

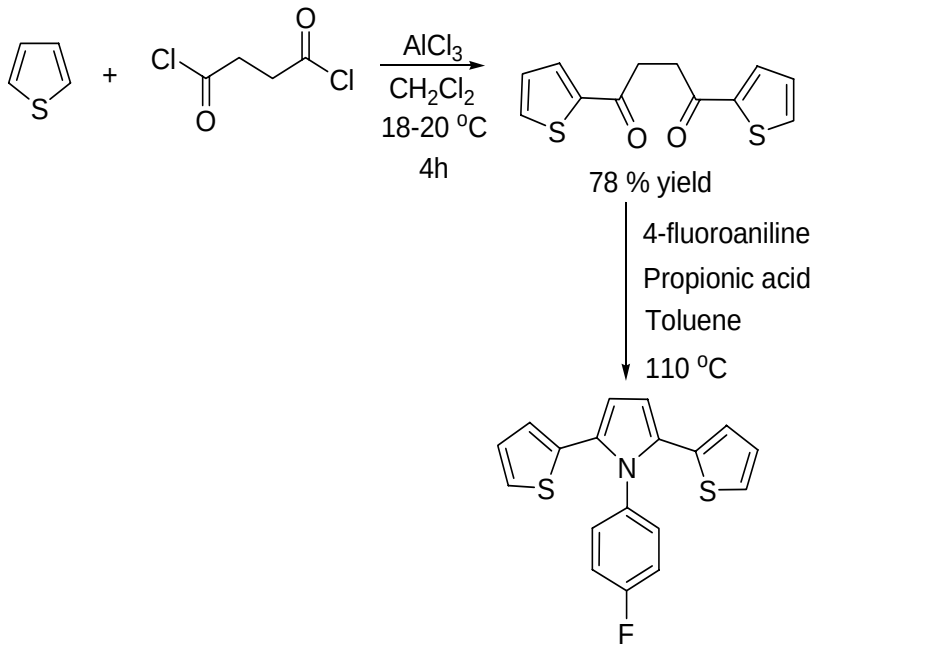

1-(4-fluorophenyl)-2,5-di(thiophen-2-yl)-1*H*-pyrrole

Figure 2.7 Synthesis route of FPTP

2.3.3 Synthesis of Conducting Copolymers of TTMT with Th and Py via Constant Potential Electrolysis

Copolymerization of TTMT with Th and was accomplished via constant potential electrolysis for 40 minutes in a two compartment cell furnished with Pt working, Pt counter, Ag reference electrodes, in the presence of 0.05 M TBAFB (supporting electrolyte), 10 mg TTMT, 80 μL Th in AN/BFEE (8:2, v/v) at 1.5 V (Figure 2.8). The freestanding polymer film was washed with AN in order to get rid of unreacted monomer. Similar procedure was applied for the synthesis of P(TTMT-co-Th) onto ITO glass working electrode in the AN/BFEE (8:2, v/v) medium containing 0.10 M TBAFB, 5 mg TTMT, 5 μL Th.

Copolymer of TTMT with Py was synthesized by application of constant potential (+1.2 V) for 40 minutes in a dual compartment electrolysis cell, described previously, in the presence of 0.05 M TBAFB, 10 mg TTMT, 70 μL Py in AN (Figure 2.9). The freestanding polymer film was washed with AN so as to get rid of unreacted monomer. Similar procedure was applied for the synthesis of P(TTMT-co-Py) onto ITO glass working electrode in the AN medium containing 0.10 M TBAFB, 5 mg TTMT, 2 μL Py.

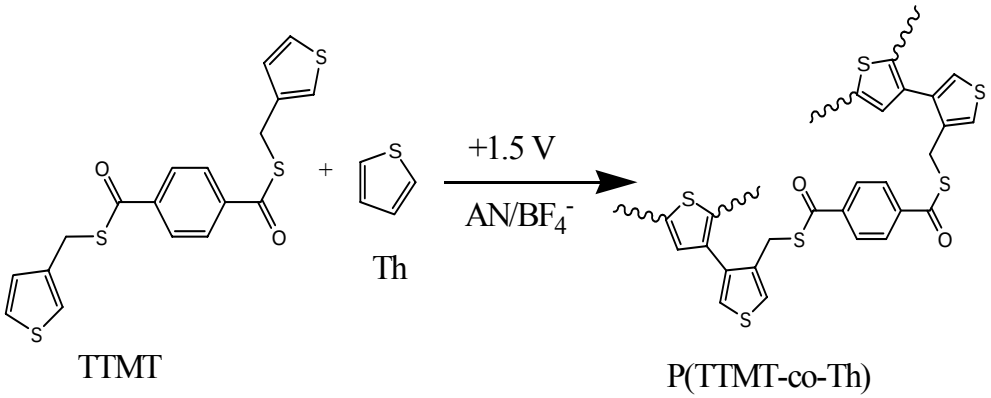

Figure 2.8 Electrochemical synthesis of P(TTMT-co-Th)

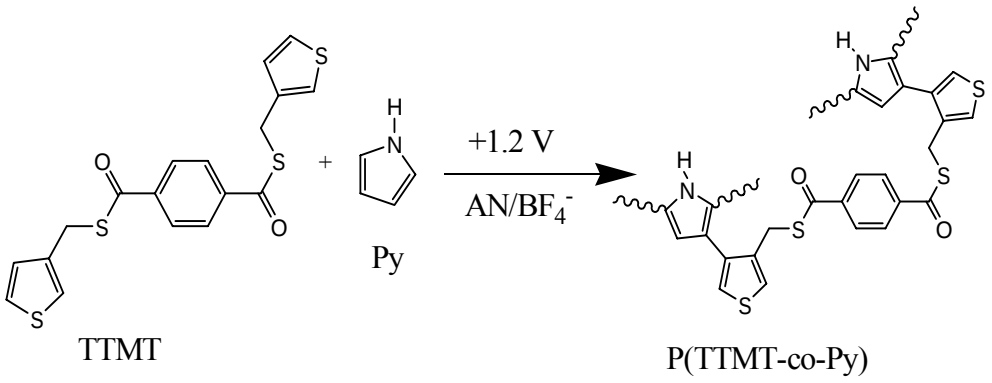

Figure 2.9 Electrochemical synthesis of P(TTMT-co-Py)

2.3.4 Oxidative Polymerization of FPTP with $FeCl_3$

0.001 g ($3.08x10^{-6}$ mol) of FPTP was polymerized using 0.0017 g ($6.15x10^{-6}$ mol) of $FeCl_3$, one of the most common oxidizing agents, in nitromethane and under nitrogen atmosphere (Figure 2.10). The reaction was carried out in ten minutes, and then methanol was added to stop the polymerization. After evaporating the solvent under vacuum, the polymer was dissolved in chloroform and the polymer solution was extracted several times with 0.1 M NaOH solution for compensation of $FeCl_3$, then the homopolymer was dried under vacuum.

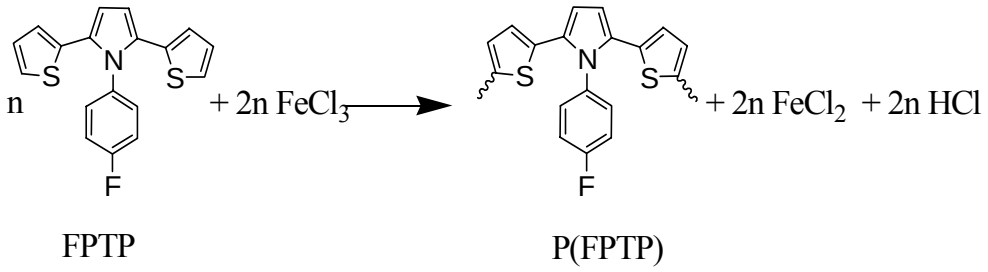

Figure 2.10 Chemical synthesis of P(FPTP)

2.3.5 Electrochemical Polymerization of FPTP

Electrochemical polymerization of FPTP was accomplished via potentiodynamic method in a two compartment cell furnished with Pt working, Pt counter, Ag reference electrodes, in the presence of 0.10 M of $NaClO_4$ and 0.10 M of $LiClO_4$ (supporting electrolyte), 5 mg FPTP in AN. Similar procedure was applied for the synthesis of P(FPTP) onto ITO glass working electrode in one compartment cell in the AN containing 0.10 M of $NaClO_4$ and 0.10 M of $LiClO_4$, 5 mg of FPTP (Figure 2.11). The electrodes coated with the polymer were washed with AN in order to get rid of unreacted monomer.

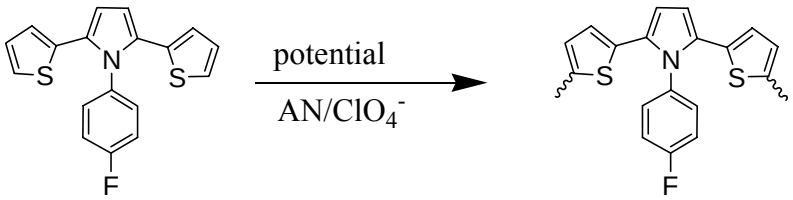

FPTP P(FPTP)

Figure 2.11 Electrochemical synthesis of P(FPTP)

2.3.6 Potentiodynamic Studies of Polymers

Oxidation/reduction behaviors of the monomers (TTMT and FPTP), the copolymers (P(TTMT-co-Th) and P(TTMT-co-Py)), and the homopolymer (P(FPTP)) were investigated via cyclic voltammetry. In all potentiodynamic studies acetonitrile was the solvent thanks to its high dielectricity and solvation power. Redox behavior of P(TTMT-co-Th) was investigated by cycling potential between 0.0 V and +2.0 V in AN/BFEE (8:2, v/v) solution containing 0.1 M of TBAFB. To determine oxidation and reduction potentials of P(TTMT-co-Py), the potential was cycled between –0.5 V and +1.5, in the

presence of 0.1 M of TBAFB. On the other hand, during the experiments carried out with FPTP, $LiClO_4$ (0.1 M)/$NaClO_4$ (0.1 M) supporting electrolyte couple was preferred and the potential was cycled between –0.25 V and +1.25 V.

2.3.7 Spectroelectrochemical Studies of Polymers

Spectroelectrochemical analyses of the two copolymers of TTMT with Th and Py, were studied by depositing the samples as thin films potentiostatically onto ITO glass. To study the spectroelectrochemistry of P(FPTP), FPTP was polymerized onto ITO glass by sweeping potential between -0.25 V and +1.25 V. Different potentials from fully reduced states of polymers to fully oxidized states were applied to the coated ITO glass slides in a monomer and also comonomer free solvent electrolyte couple, while spectroelectrochemical series were taken at the same time. The types and concentrations of electrolytes were same as those in electrolysis solutions.

2.3.8 Switching Properties of Polymers

A remarkable color change and the switching ability between the two colored states of the polymer are crucially important for electrochromic applications. A square wave potential step method, coupled with optical spectroscopy known as chronoabsorptometry was used to probe switching time and contrast. During the experiments, the copolymers and the homopolymer coated onto ITO glass were switched at the wavelength of maximum contrast between its neutral and doped states for five seconds and % transmittance (%T) was measured. P(TTMT-co-Th), P(TTMT-co-Py) and P(FPTP) were switched by application of 0.0 V and +1.2V, -0.6 V and +0.8 V, -0.6 V and +1.0 V, respectively.

2.3.9 Electrochromic Device (ECD) Construction

Electrochromic devices (ECDs) were constructed by sandwiching the gel electrolyte between anodically and cathodically coloring polymers, which were electrochemically deposited onto ITO coated glass electrodes, as shown in Figure 2.12. Cathodically coloring polymers ((P(TTMT-co-Th), P(TTMT-co-Py), P(FPTP)) were coated onto glass electrodes as described previously. In construction of P(TTMT-co-Th)/PEDOT and P(TTMT-co-Py)/PEDOT electrochromic devices, anodically coloring polymer, PEDOT, was deposited from 0.10 M TBAFB/AN electrolyte containing 3 μL EDOT; on the other hand, to construct P(FPTP)/PEDOT ECD 3 μL EDOT was dissolved in AN containing 0.1 M $LiClO_4$ and 0.1 M $NaClO_4$ (Figure 2.13). The redox sites of the polymer films were matched by the employment of chronocoulometry so as to attain effective switching. The anodically coloring polymers were completely reduced, whereas PEDOT was completely oxidized in monomer free solvent/supporting electrolyte system before assembling the ECDs.

2.3.10 Preparation of Gel Electrolyte

The fully transparent and highly conducting gel electrolyte was prepared by plasticization of PMMA with 1, 2-propylenecarbonate in TBAFB/AN medium. The blend was heated at 70ºC and continuously stirred until gel formation. The ratio of the composition of TBAFB/PMMA/PC/AN was 3:7:20:70. The gel electrolyte prepared by this way was used in the construction of P(TTMT-co-Th)/PEDOT and P(TTMT-co-Py)/PEDOT ECDs; however, to assemble P(FPTP)/PEDOT ECD in place of TBAFB, $LiClO_4$ and $NaClO_4$ were utilized by changing the gel electrolyte composition to $LiClO_4$/$NaClO_4$/PMMA/PC/AN: 1.5:1.5:7:20:70.

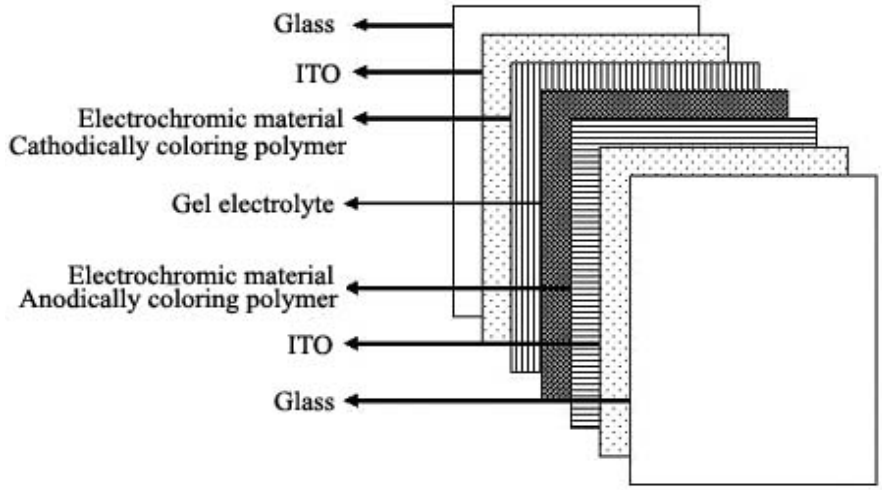

Figure 2.12 Schematic representation of an ECD

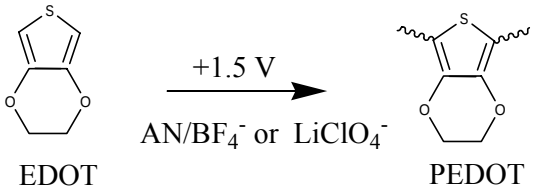

Figure 2.13 Electrochemical synthesis of PEDOT

2.3.11 Spectroelectrochemical Studies of ECDs

The characterization of the devices, optical properties was carried out using a Agilent 8453 UV-Vis spectrophotometer. A device without the electrochromic polymer layer, but otherwise with the same assembly, was used as a reference. In order to apply voltage across the device, the counter and the reference leads are connected to one another.

Spectroelectrochemistry analysis was obtained by sequentially stepping the applied potential. While measuring the absorbance as a function of wavelength, the P(TTMT-co-Th)/PEDOT, P(TTMT-co-Py)/PEDOT,

P(FPTP)/PEDOT devices switched at voltages varying between 0.0 V and +2.6 V, -2.4 V and +0.8 V, -0.8V and +1.1V, respectively.

2.3.12 Switching Properties of ECDs

Switching properties of devices were investigated by application of potential square wave technique with a residence time of 5 seconds at the switching voltages, which were 0.0 V and +2.6 V for P(TTMT-co-Th)/PEDOT ECD, -2.4 V and +0.8 V for P(TTMT-co-Py)/PEDOT ECD, -0.8 V and +1.1 V for P(FPTP)/PEDOT ECD.

2.3.13 Open Circuit Memory Studies of ECDs

As stated by Girotto et al. the color persistence in the ECDs is an important feature since it is directly related to aspects involved in its utilization and energy consumption during use [78]. The optical memory of an electrochromic material is defined as the time during which this material retains its color without applying potential [79]. In the experiment, the ECD was polarized in the undoped/doped states by an applied pulse for 1 second and then kept under open circuit conditions for 199 seconds while the optical spectrum at certain wavelength as a function of time was monitored. Memory effect of P(TTMT-co-Th)/PEDOT ECD was examined by application of 0.0 V and +2.6 V as a pulse at 636 nm. Open circuit memory of P(TTMT-co-Py)/PEDOT ECD, was tested at –2.4 V, 0.0 V and +2.6 V at 580 nm. Applied pulses of -0.8 V, 0.0 V, +1.1 V at 615 nm polarized P(FPTP)/PEDOT ECD.

2.3.14 Stabilities of ECDs

Construction of ECDs with long life times is targeted in electrochromic applications. In order to evaluate redox stability of the device under atmospheric conditions, cyclic voltammetry was utilized. The voltages of the

devices were repeatedly swept between 0.0 V and +2.6 V, -2.0 V and +2.5 V, -0.5 V and +2.0 V for P(TTMT-co-Th)/PEDOT ECD, P(TTMT-co-Py)/PEDOT ECD, P(FPTP)/PEDOT ECD, respectively with 500 mV/s scan rate while monitoring cyclic voltammetry.

2.3.15 Colorimetry Measurements

Colorimetry analysis, which enables numeric determination of color, is considered as a valuable method for electrochromic applications. The commonly utilized scale was set by La Commission Internationale de l'Eclairage (CIE). In CIE system, luminance or brightness, hue and saturation, symbolized with L, a, b respectively, are determined to qualify color. L, a, b values of the copolymer and homopolymer films as well as the devices were measured at switching voltages.

CHAPTER III

RESULTS AND DISCUSSION

3.1 Synthesis of TTMT and Its Copolymers with Thiophene and Pyrrole and Their Characterization

3.1.1 Characterization of TTMT with NMR Spectroscopy

NMR spectra of monomer were taken by using $CDCl_3$ as the solvent and chemical shifts (δ) are given relative to tetramethylsilane as the internal standard.

^{1}H-NMR (δ, ppm) data (Figure 3.1) for TTMT: 4.4 (s, 4H, methyl), 7.1 (2H, 5-thienyl), 7.3 (m, 2- and 4- thienyl), 8 (s, 4H, phenyl).

^{13}C-NMR (δ, ppm) data (Figure 3.2) for TTMT: 28.2 (C_e), 123.3 (C_d), 126.3 (C_a), 127.5 (C_b), 128.1 (C_h), 136.9 (Cc), 140.4 (C_g), 190.5 (C_f).

3.1.2 FTIR Spectra of TTMT, P(TTMT-co-Th) and P(TTMT-co-Py)

In the FTIR spectrum of monomer (Figure 3.3 a) the following absorption peaks were identified: 2921 cm^{-1} and 2851 cm^{-1} (aliphatic methylene stretching vibration), 1657 cm^{-1} (C=O stretching vibration arising from carbonyl sandwiched between an aryl group and sulfur), 1202 cm^{-1} (C-C stretching vibration arising from carbonyl bonded to an aryl group), 1107 cm^{-1} (thienyl C=C stretching vibration), 903 cm^{-1} (C-S stretching vibration due to

carbonyl bonded to sulfur). The absorption bands at 1495, 838, 784, 652 cm^{-1} were due to the vibrations of C-H and C=C bonds of thiophene rings. The peaks at 838 cm^{-1} and 784 cm^{-1} were related to the β-hydrogen and α-hydrogen of thiophene ring, respectively.

The FTIR spectrum (Figure 3.3.b) revealed that TTMT was successfully electrocopolymerized with Th. The peak monitored at 838 cm^{-1} indicating C-H_β vibration of the thiophene ring and the band at 652 cm^{-1} due to deformations of C-H out of plane of the thiophene ring disappeared completely upon polymerization, in other words TTMT was polymerized from its 4- position. The strong peak observed at 1086 cm^{-1} showed the presence of BF_4^- dopant ion in the polymer matrix. The medium and broad peak monitored at 1633 cm^{-1} was the C=O stretching vibration arising from carbonyl sandwiched between an aryl group and sulfur indicating the presence of carbonyl group after polymerization.

The FTIR spectrum (Figure 3.3 c) revealed that electrocopolymerization of TTMT with Py was successfully realized. The peak monitored at 838 cm^{-1} indicating C-H_β of the thiophene ring of the thiophene ring disappeared completely upon polymerization. The peaks observed at 1513 cm^{-1} and 1158 cm^{-1} were due to pyrrole N-H and C-N stretching vibrations, respectively and they showed the presence of pyrrole in the polymeric matrix. In addition, the new peaks formed at 1034 cm^{-1}, 878 cm^{-1}, 1117 cm^{-1} were attributed to N-H and C-H deformation vibrations of three neighboring H atoms of 2-substituted pyrrole. The strong peak observed at 1082 cm^{-1} was the characteristic BF_4^- dopant ion peak. The medium and broad peak monitored at 1647 cm^{-1} was the C=O stretching vibration arising from carbonyl sandwiched between an aryl group and sulfur and the intensity of that peak was relatively low when compared to the intensity of the carbonyl peak of the monomer.

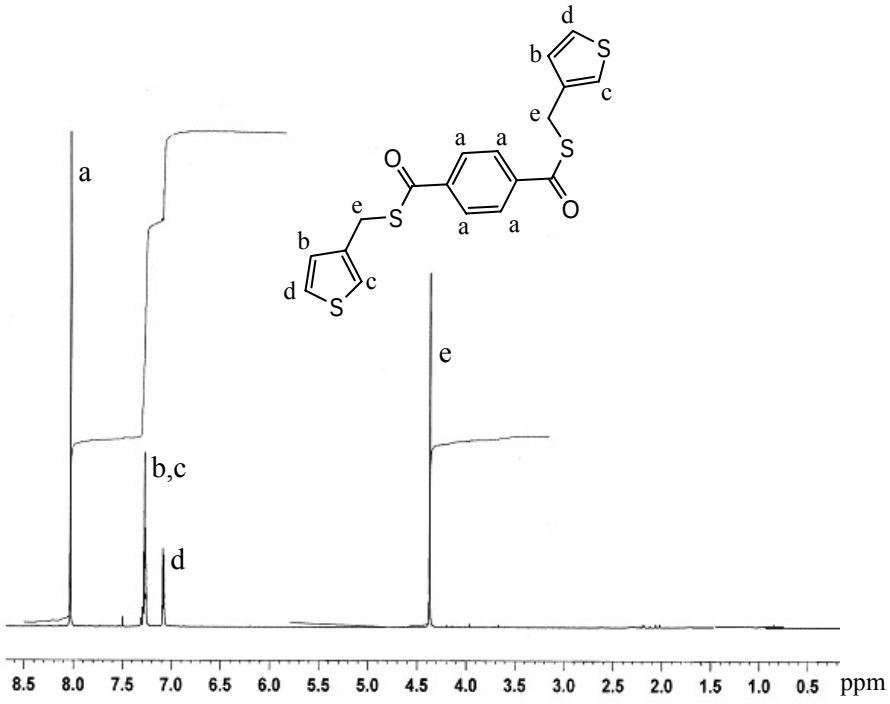

Figure 3.1 [1]H-NMR spectrum of TTMT

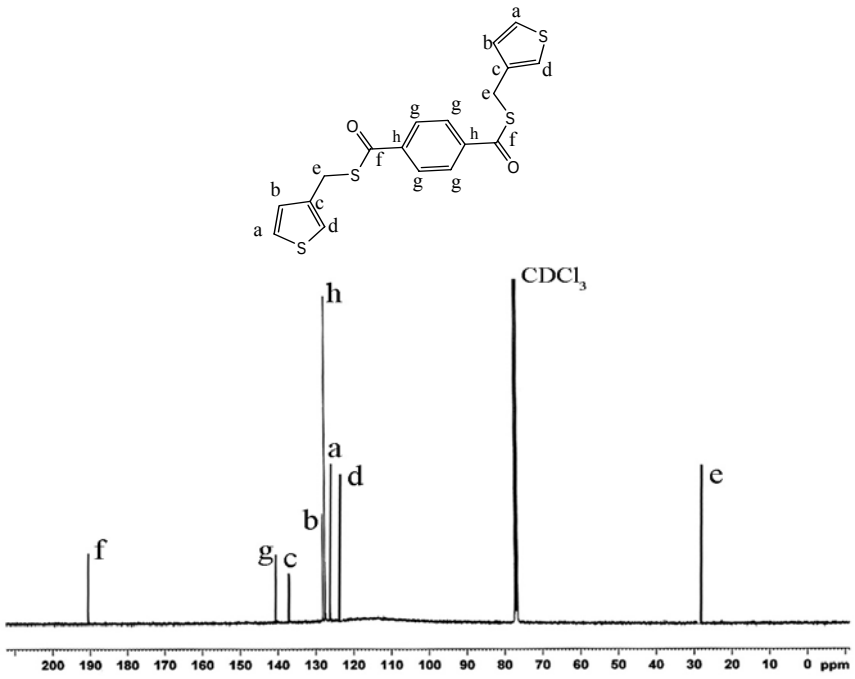

Figure 3.2 [13]C-NMR spectrum of TTMT

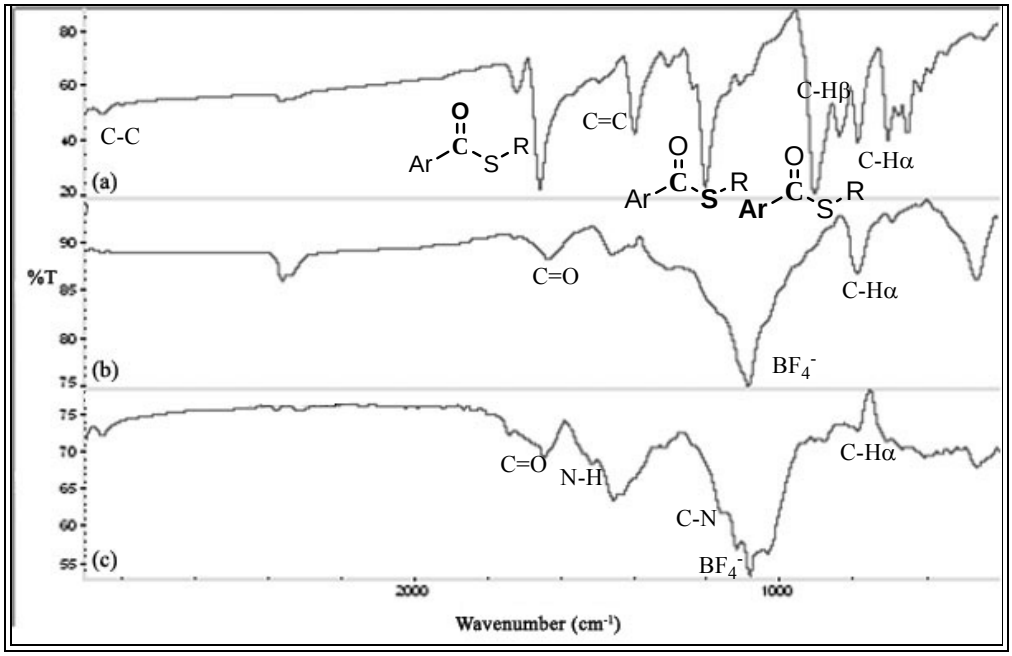

Figure 3.3 FTIR spectra of (a) TTMT, (b) P(TTMT-co-Th), (c) P(TTMT-co-Py)

3.1.3 Cyclic Voltammograms of P(TTMT-co-Th) and P(TTMT-co-Py)

Oxidation-reduction behavior of TTMT was investigated via cyclic voltammetry. Cyclic voltammograms taken in AN/TBAFB, AN/BFEE/TBAFB and BFEE/TBAFB media revealed that the monomer was not electroactive since it was lacking any redox peaks. Upon addition of thiophene into AN/BFEE/TBAFB medium, a reversible electroactivity different than that of Th was observed (Figure 3.4). In the cyclic voltammogram of PTh shown in Figure 3.4 a +0.5 V and +0.9 V were observed as the reduction and oxidation peaks respectively; on the other hand, Figure 3.4 b revealed that P(TTMT-co-Th) had +0.75 V as the reduction and +1.1 V as the oxidation potential. Oxidation-reduction behavior of TTMT in the presence of Py was also investigated via cyclic voltammetry and upon sequential cycling; there was a gradual film formation, indicated by the continuous increase in the current intensity (Figure 3.5). In the cyclic

voltammogram of PPy shown in Figure 3.5 a PPy has well defined reduction peak at –0.18 V and oxidation peak at +0.25 V; on the other hand, Figure 3.5 b revealed that P(TTMT-co-Py) had –0.13 V as the reduction and 0.4 V as the oxidation potential.

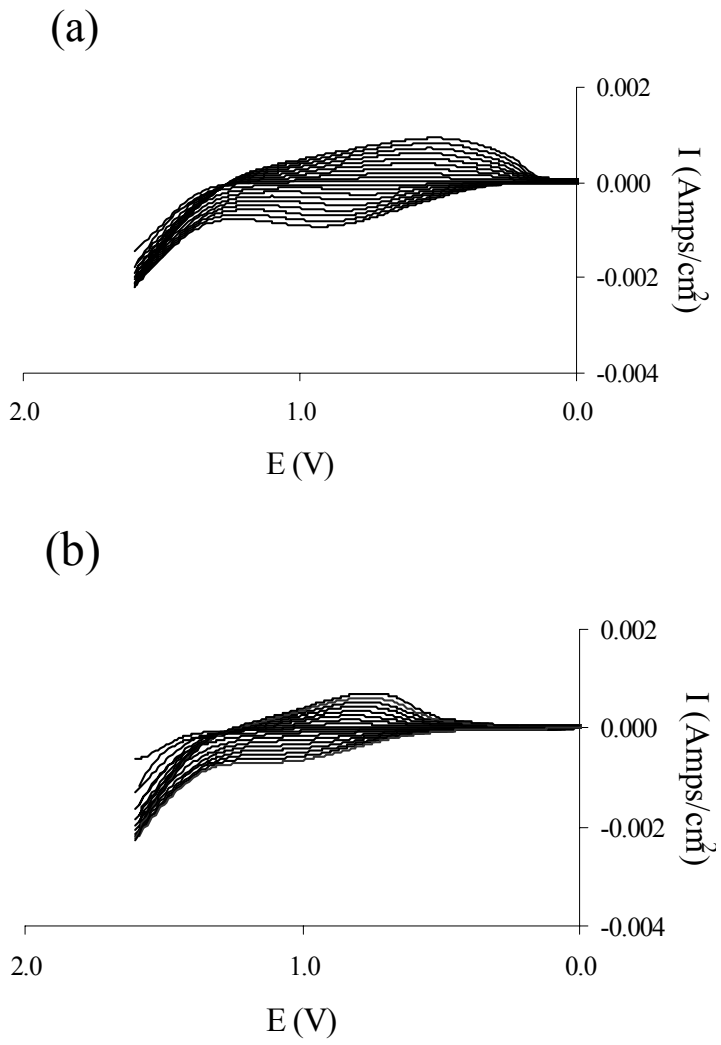

Figure 3.4 Cyclic voltammograms of (a) PTh, (b) P(TTMT-co-Th)

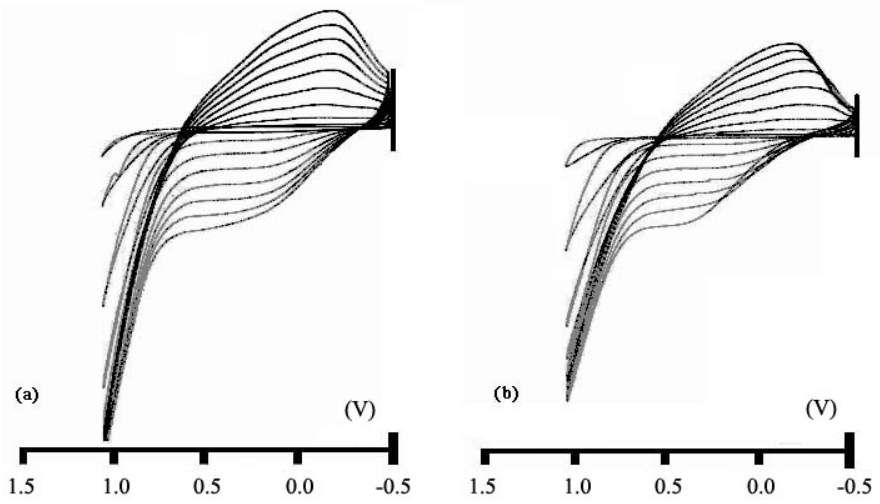

Figure 3.5.Cyclic voltammograms of (a) PPy, (b) P(TTMT-co-Py)

3.1.4 Thermal Analysis of TTMT, P(TTMT-co-Th) and P(TTMT-co-Py)

Melting point of TTMT was found as 110 ˚C. Thermal behavior of TTMT copolymers with Th and Py were examined with DSC in the range of 25 ˚C-350 ˚C at a heating rate of 10 ˚C per minute under N_2 atmosphere (Figure 3.6). The removal of solvent was observed at 106.97 ˚C for P(TTMT-co-Th), whereas the dopant ion was removed at around 225 ˚C. In the case of P(TTMT-co-Py) removals of solvent and dopant ion were viewed at 83.04 ˚C and 258.59 ˚C, respectively.

3.1.5 Morphologies of P(TTMT-co-Th) and P(TTMT-co-Py) Films

Both SEM micrographs of P(TTMT-co-Th) were different compared to pure polythiophene films. Solution side of PTh film has a very characteristic cauliflower like structure; with a smooth surface on the electrode side, on the other hand, solution side of P(TTMT-co-Th) film showed a worm like structure whereas electrode side had a rough surface (Figures 3.7 a and b, respectively). In the case of P(TTMT-co-Py) also, the morphologies of both

sides of the film were different in comparison to pure PPy. Solution side of PPy has a much defined shaped cauliflower like structure; with a smooth surface on the electrode side; conversely, solution side of P(TTMT-co-Py) had a granular structure and the surface of the electrode side was rough (Figures 3.8.a and b, respectively).

3.1.6 Conductivities of P(TTMT-co-Th) and P(TTMT-co-Py) Films

Room temperature (20 ºC) conductivities of the polymer films were measured via four-probe technique and the results were summarized in Table 3.1. Conductivity of P(TTMT-co-Th) was determined as $1.1x10^{-2}$ S/cm; on the other hand, the conductivity of the pure polythiophene film, which was synthesized at the same conditions, was measured as 3.3 S/cm. Conductivity of P(TTMT-co-Py) was found to be 0.60 S/cm, and that of pure PPy was found to be 1.1 S/cm. For both copolymers, conductivities of the solution sides and electrode sides were in the same order of magnitude, revealing the homogeneity of the films in terms of conductivity. The fact that the conductivity of the copolymer films were less than that of the pure polythiophene and polypyrrole films can be explained by weakening of conjugation through TTMT units and considered as a proof of copolymerization.

Table 3.1 Conductivities of PTh, P(TTMT-co-Th), PPy, P(TTMT-co-Py) films

	Conductivities (S/cm)
PTh	3.3
P(TTMT-co-Th)	$1.1x10^{-2}$
PPy	1.1
P(TTMT-co-Py)	0.6

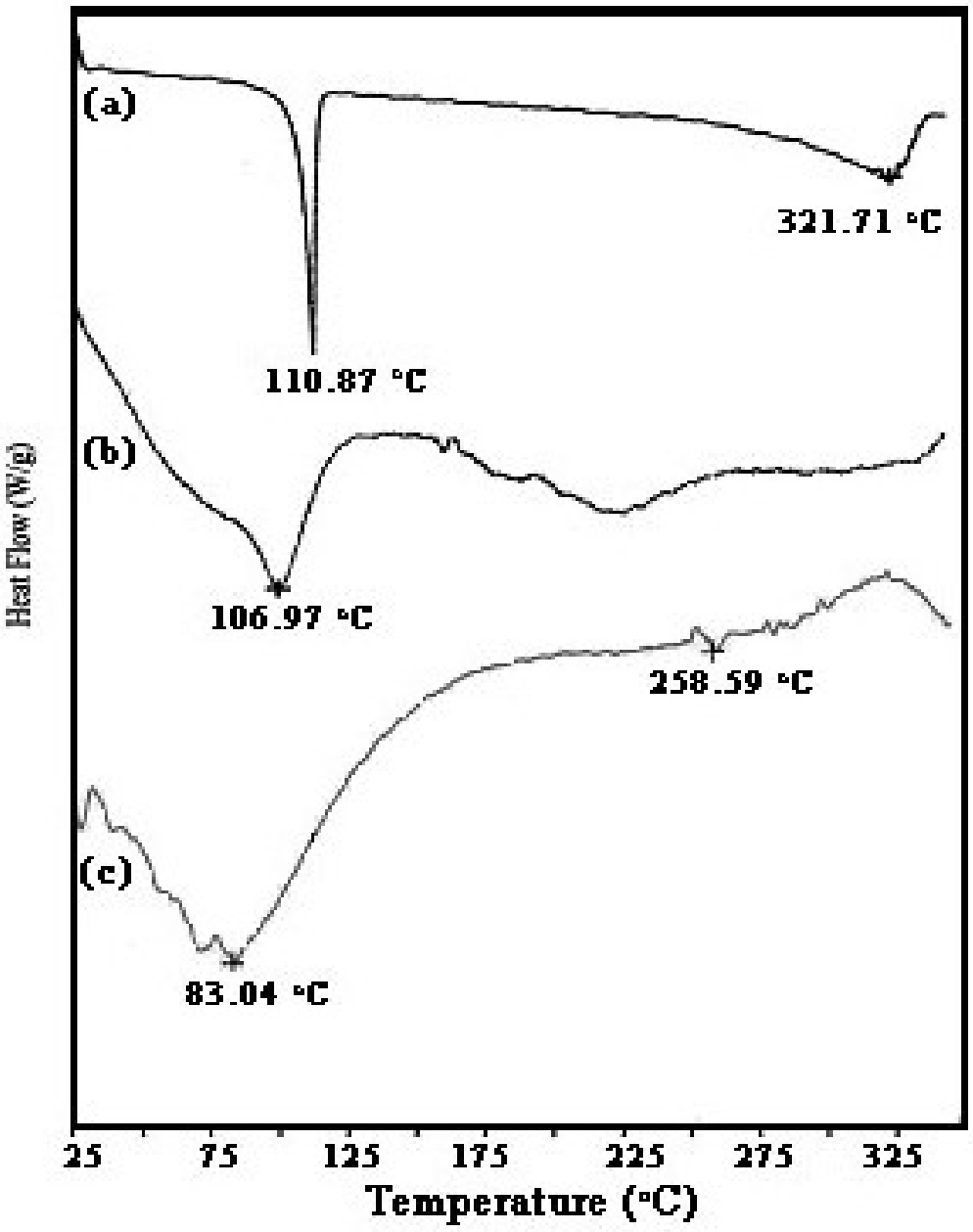

Figure 3.6 DSC thermograms of (a) TTMT, (b) P(TTMT-co-Th), (c) P(TTMT-co-Py)

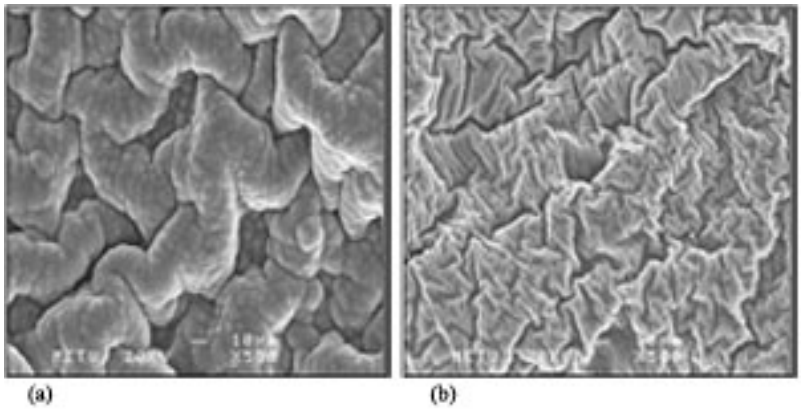

Figure 3.7 SEM pictures of (a) solution side of P(TTMT-co-Th), (b) electrode side of P(TTMT-co-Th)

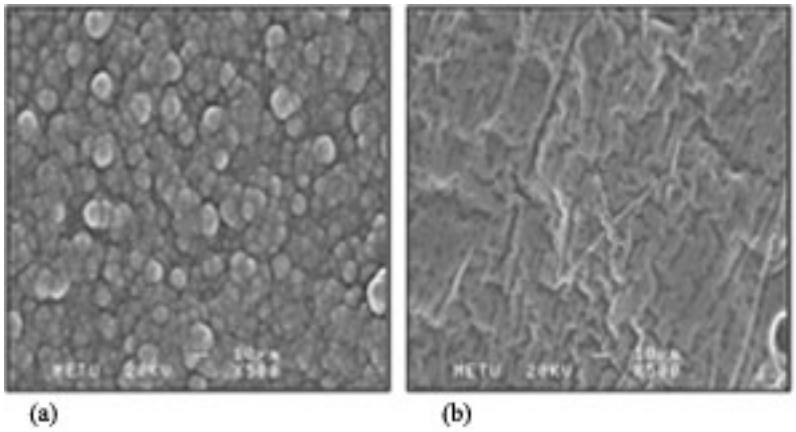

Figure 3.8 SEM pictures of (a) solution side of P(TTMT-co-Py), (b) electrode side of P(TTMT-co-Py)

3.1.7 Spectroelectrochemistry Studies of P(TTMT-co-Th) and P(TTMT-co-Py)

TTMT was potentiostatically copolymerized with Th and Py onto an ITO glass in solvent/supporting electrolyte mixture. The copolymer deposited ITO glasses were put in a monomer free environment and spectroelectrochemical properties were determined. Spectroelectrochemical analyses of P(TTMT-co-Th) and P(TTMT-co-Py) were done with the purpose of elucidating electronic

transitions and change in optical properties upon redox switching. Optoelectrochemical spectra of P(TTMT-co-Th) as a function of applied voltage are given in Figure 3.9 revealing λ_{max} as 476 nm with a band gap of 2.0 eV. The absorptions observed at around 750 nm and 820 nm were attributed to the evolution of polaron and bipolaron bands, respectively (Figure3.10). For P(TTMT-co-Py), at the reduced state λ_{max} due to π to π^* state transition was found to be 375 nm and band gap energy was calculated as 2.4 eV (Figure 3.11). Appearance of peaks around 725 nm and 930 nm could be attributed to the evolution of polaron and bipolaron bands respectively (Figure 3.12).

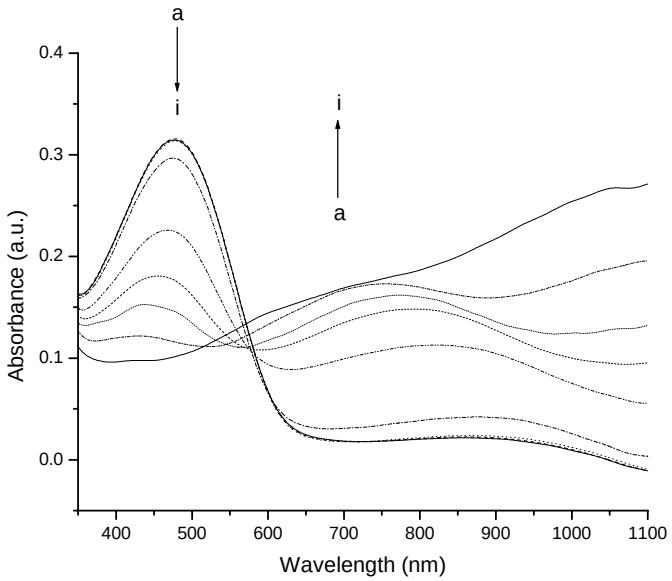

Figure 3.9 Spectroelectrochemistry of P(TTMT-co-Th) as a function of wavelength (300 nm-1100 nm) at applied potentials between 0.0 V and +1.2 V: (a) 0.0 V, (b) +0.2 V, (c) +0.4 V, (d) +0.6 V, (e) +0.7 V, (f) +0.8 V, (g) +0.9 V, (h) +1.0 V, (i) +1.2 V.

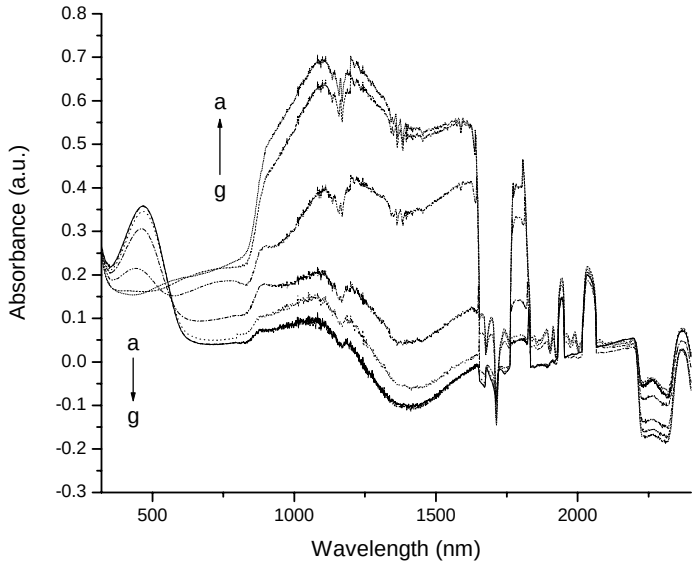

Figure 3.10 Spectroelectrochemistry of P(TTMT-co-Th) as a function of wavelength (300nm-2400nm) at applied potentials between 0.0 and +1.2 V: (a) 0.0 V, (b) +0.2 V, (c) +0.4 V, (d) +0.6 V, (e) +0.8 V, (f) +1.0 V, (g) +1.2 V.

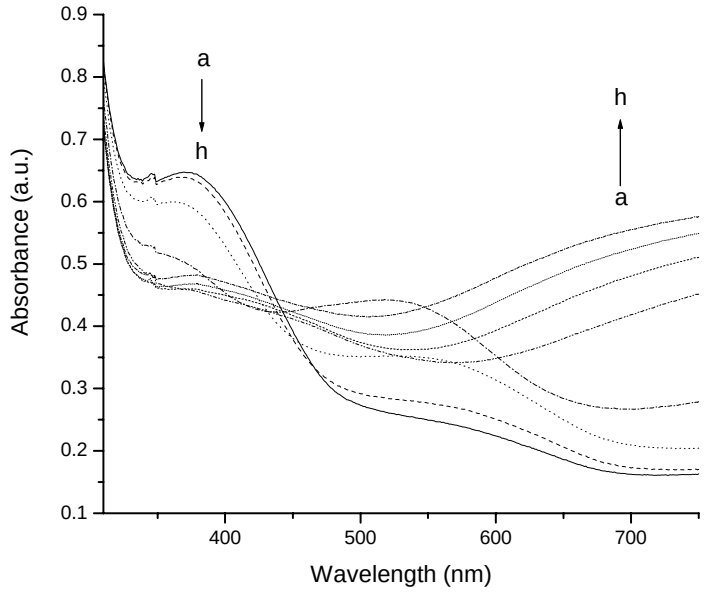

Figure 3.11 Spectroelectrochemistry of P(TTMT-co-Py) as a function of wavelength (300 nm-700 nm) at applied potentials between –0.6 and +0.8 V: (a) –0.6 V, (b) –0.4 V, (c) –0.2 V, (d) 0.0 V, (e) +0.2 V, (f) +0.4 V, (g) +0.6 V, (h) +0.8 V.

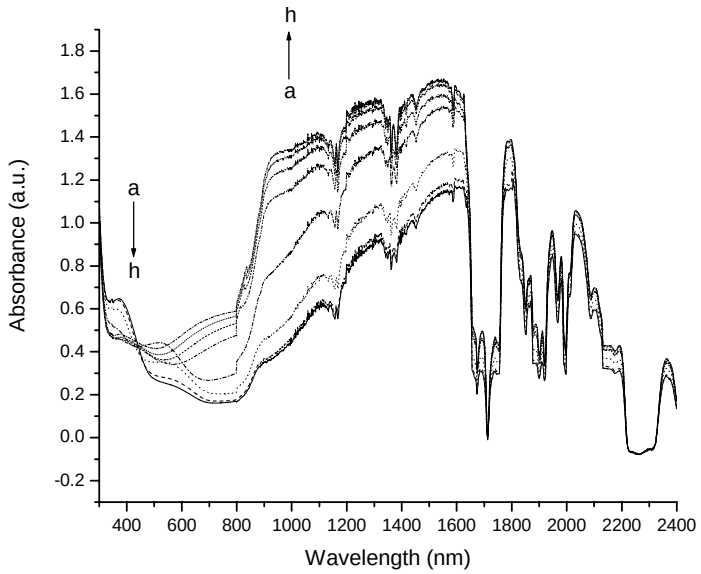

Figure 3.12 Spectroelectrochemistry of P(TTMT-co-Py) as a function of wavelength (300 nm-2500 nm) at applied potentials between –0.6 V and +0.8 V: (a) –0.6 V, (b) –0.4 V, (c) -0.2 V, (d) 0.0 V, (e) +0.2 V, (f) +0.4 V, (g) +0.6 V, (h) +0.8 V.

3.1.8 Colorimetry Measurements for P(TTMT-co-Th) and P(TTMT-co-Py)

Colorimetry analysis, which enables numeric determination of color, is considered as a valuable method for electrochromic applications. The commonly utilized scale was set by La Commission Internationale de l'Eclairage (CIE). In CIE system, luminance or brightness, hue and saturation, symbolized with L, a, b respectively, are determined to qualify color. At the fully reduced state the color of P(TTMT-co-Th) was brown (L=45, a=17 b=29); on the other hand, at the fully oxidized state the film has a blue color (L=57, a=-4, b=4) (Figure 3.13). At the fully reduced state P(TTMT-co-Py) was greenish yellow (L=74, a=-10, b=89), at 0.0 V the color of the polymer turned to red (L=68.4, a=16.0, b=-7.1); on the other hand, at the fully oxidized state the film has a greenish blue color (L=40.3, a=-16.2, b=-16.1) (Figure

3.14). The results are summarized in Table 3.2 for P(TTMT-co-Th) and P(TTMT-co-Py.

Table 3.2 Colors of P(TTMT-co-Th) and P(TTMT-co-Py) films

Material	Eg (eV)	Color	L	a	b
P(TTMT-co-Th)	2	Brown	45	17	29
		Blue	57	-4	4
P(TTMT-co-Py)	2.4	Greenish yellow	74	68	40
		Red	-10	16	-16
		Greenish blue	89	-7	-16

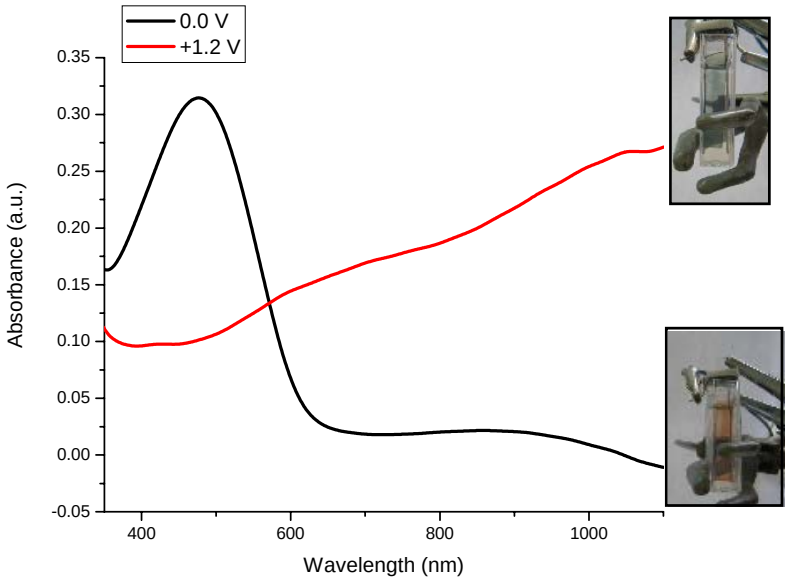

Figure 3.13 Colors of P(TTMT-co-Th) at different switching voltages

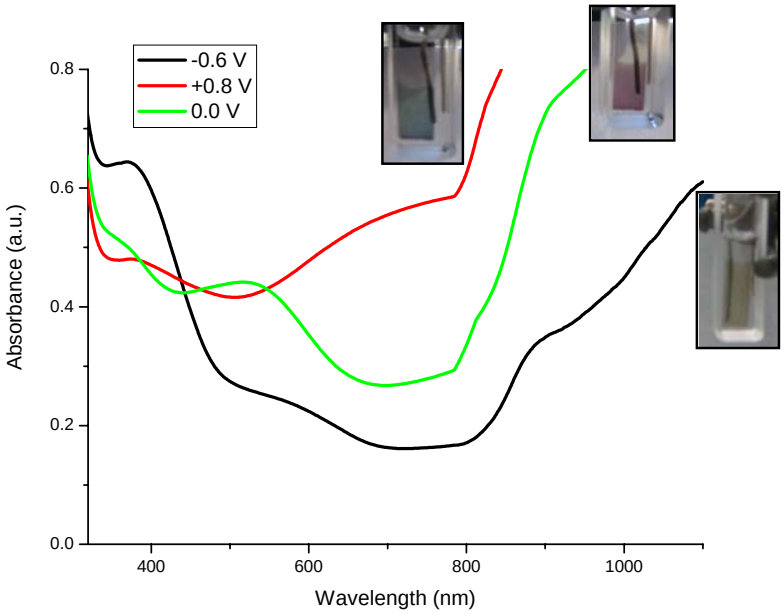

Figure 3.14 Colors of P(TTMT-co-Py) at different switching voltages

3.1.9 Switching Properties of P(TTMT-co-Th) and P(TTMT-co-Py)

During the experiment, P(TTMT-co-Th) coated onto ITO glass was switched at 476 nm by application of 0.0 V and +1.2 V respectively, for five seconds and % Transmittance (%T) was measured. For P(TTMT-co-Th), optical contrast (%ΔT) and switching were calculated as 16% and 1.3 s respectively at 476 nm. P(TTMT-co-Py) was switched between –0.6 V and +0.8 V, optical contrast (%ΔT) plus switching time were calculated as 4.6% and 1.7 s respectively at the given λmax. However, the maximum contrast in the visible range was found as 13% at 725 nm, at that wavelength, switching time was calculated as 1.45 s. Figure 3.15 and Figure 3.16 show transmittance-time profiles of the copolymers with Th and Py, respectively, recorded during the experiment.

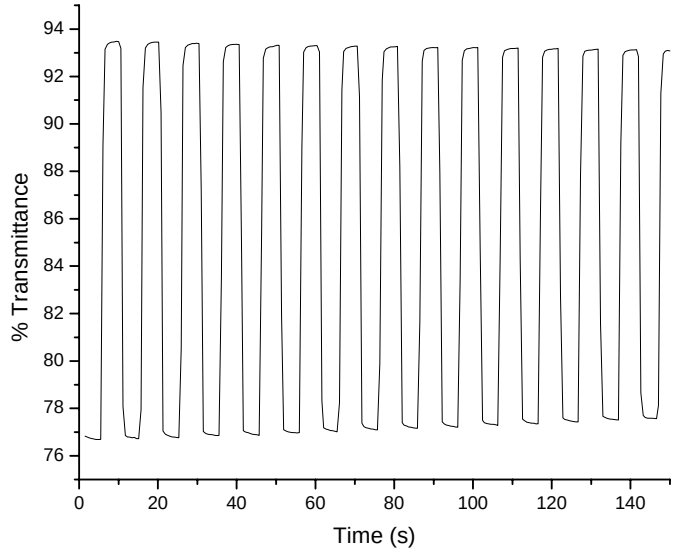

Figure 3.15 Electrochromic switching, optical absorbance change monitored at 476 nm for P(TTMT-co-Th) between 0.0 V and +1.2 V.

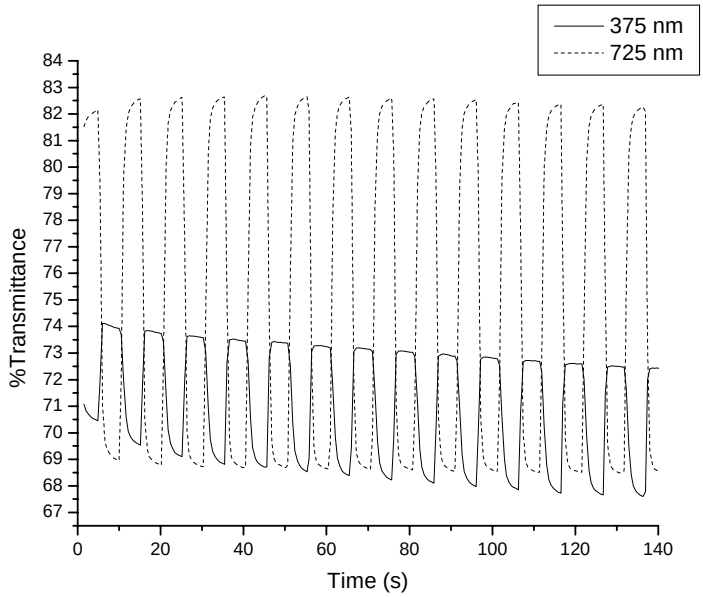

Figure 3.16 Electrochromic switching, percent transmittance change monitored at 375 nm (solid line) and 725 nm (dashed line) for P(TTMT-co-Py) between -0.6 V and +0.8 V.

3. 2 Characterization of P(TTMT-co-Th)/PEDOT Device

3.2.1 Spectroelectrochemistry of P(TTMT-co-Th)/PEDOT Device

With the aim of examining optical changes of the ECDs occurring upon doping and dedoping, spectroelectrochemical studies were carried out. Figure 3.17 shows the spectra of P(TTMT-co-Th)/PEDOT device at voltages varying between 0.0 V and +2.6 V. Upon stepwise increase of the applied potential from 0.0 V to +2.6 V, alternation of the color from brown to blue was observed. When 0.0 V bias was applied to the P(TTMT-co-Th), anodically coloring polymer layer, brown color was observed. There was a maximum absorption at 446 nm due to π to π^* electronic transition. At this potential, the PEDOT layer was in oxidized state, revealing a transparent sky blue color and the color of the ECD was dominated by the copolymer, which was in its neutral state. At potentials beyond +0.8 V, the PEDOT starts to dominate and evaluation of a new peak at around 636 nm due to π to π^* transition was monitored. With the application of +2.6 V, the copolymer was fully oxidized whereas, the PEDOT layer was in its neutral state, and thus, at this voltage the color of the ECD was blue.

3.2.2 Colorimetry Measurements of P(TTMT-co-Th)/PEDOT Device

When 0.0 V bias was applied to the P(TTMT-co-Th), anodically coloring polymer layer, the copolymer was completely reduced and the ECD has brown color (L=49, a=5, b=25). With the application of +2.6 V, the copolymer was entirely oxidized whereas the PEDOT layer was in its neutral state, at this voltage the color of the ECD was blue (L=52, a=0, b=-28). Figure 3.18 shows the change in color with application of switching voltages.

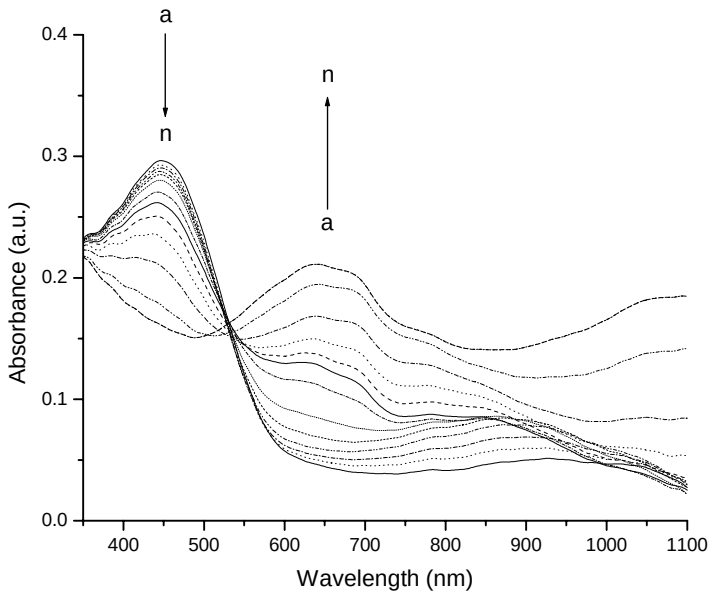

Figure 3.17 Spectroelectrochemistry of P(TTMT-co-Th)/PEDOT device as a function of wavelength at applied potentials between 0.0 and +2.6 V: (a) 0.0 V, (b) +0.2 V, (c) +0.4 V, (d) +0.6 V, (e) +0.8 V, (f) +1.0 V, (g) +1.2 V, (h) +1.4 V, (i) +1.6 V, (j) +1.8 V, (k) +2.0 V, (l) +2.2 V, (m) +2.4 V, (n) +2.6 V.

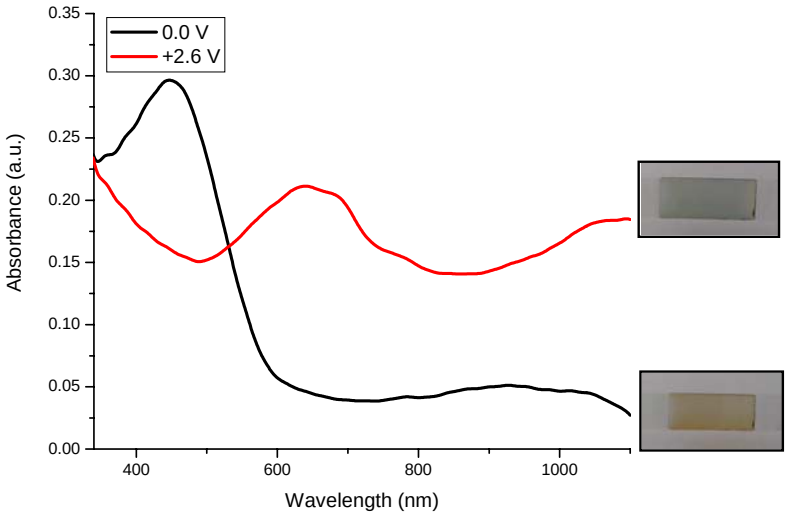

Figure 3.18 Colors of P(TTMT-co-Th)/PEDOT device at different switching voltages

3.2.3 Switching Properties of P(TTMT-co-Th)/PEDOT Device

The response time needed to perform switching between the two colored states and the optical contrast were determined for P(TTMT-co-Th)/PEDOT device. In this double potential step experiment, the potential was stepped between 0.0 V and +2.6 V with a residence time of five seconds at each potential. The optical contrast, monitored at 636 nm, was measured as 11% and the switching time was calculated as 1.1 s at the maximum transmittance. Figure 3.19 shows transmittance-time profiles of the ECD recorded during the experiment.

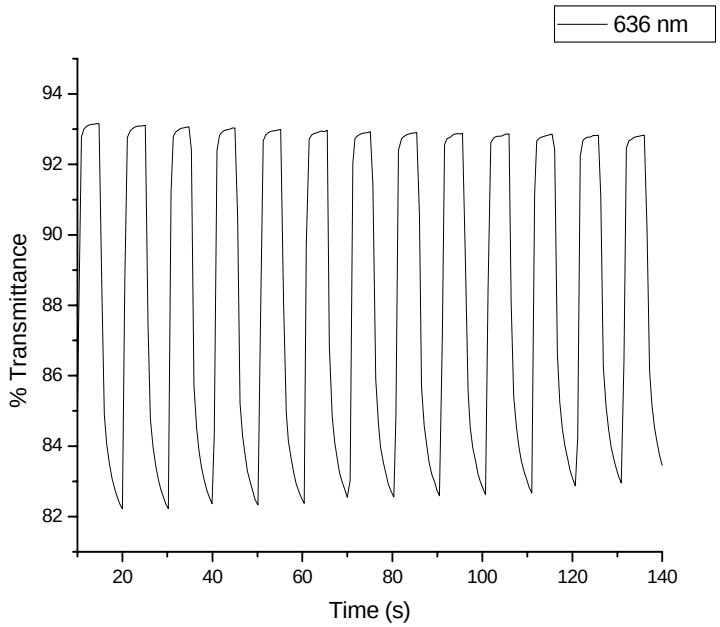

Figure 3.19 Electrochromic switching, optical absorbance change monitored at 636 nm for P(TTMT-co-Th)/PEDOT device between 0.0 V and +2.6 V.

3.2.4 Open Circuit Memory of P(TTMT-co-Th)/PEDOT Device

In the experiment the ECD was polarized in the brown/blue states by an applied pulse (0.0 V/+2.6 V, brown/blue colored states, respectively) for 1 second and then kept under open circuit conditions for 199 seconds while the optical spectrum at 636 nm as a function of time was monitored (Figure 3.20). When polarized upon application of +2.6 V in the blue colored state, %T abruptly changed to 83%, whereas during 199 seconds the ECD tried to reach 85% transmittance, in other words it was able to remember its color.

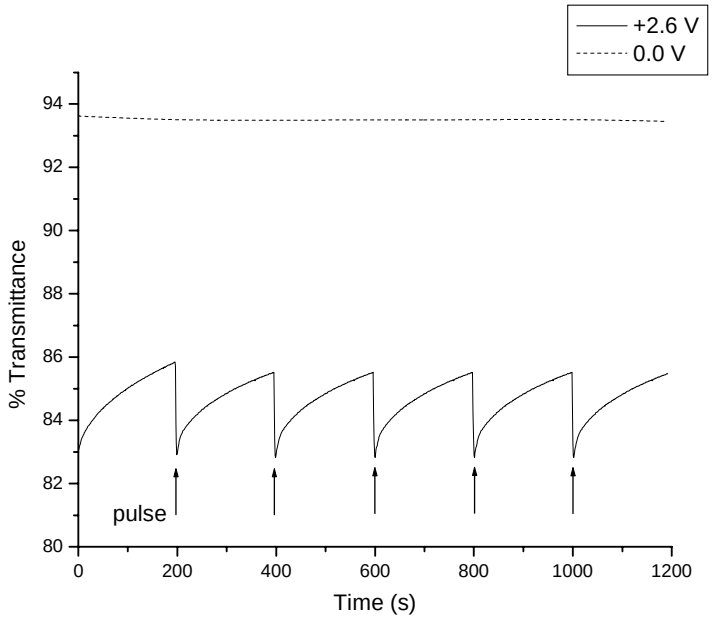

Figure 3.20 Open circuit memory of P(TTMT-co-Th)/PEDOT device monitored by single-wavelength absorption spectroscopy at 636 nm. 0.0 V (dashed line) and +2.6 V (solid line) pulse are applied for 1 s every 200 s to recover the initial transmittance.

3.2.5 Stability of P(TTMT-co-Th)/PEDOT Device

In order to evaluate redox stability of the device under atmospheric conditions, cyclic voltammetry was utilized. The voltage of the device was continuously swept between 0.0 V and +2.6 V with 500 mV/s scan rate and cyclic voltammetry was monitored (Figure 3.21). As seen in the figure mentioned, P(TTMT-co-Th)/PEDOT could be repeatedly switched up to 500 cycles retaining most (70%) of its electroactivity.

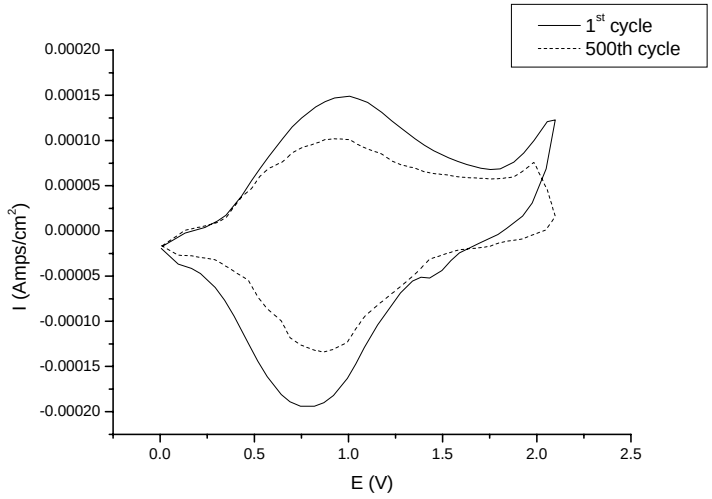

Figure 3.21 Cyclic voltammogram of P(TTMT-co-Th)/PEDOT device as a function of repeated scans 500 mV/s: after 1 cycle (solid line), after 500 cycles (dashed line).

3.3 Characterization of P(TTMT-co-Py)/PEDOT Device

3.3.1 Spectroelectrochemistry of P(TTMT-co-Py)/PEDOT Device

The optoelectronic spectra of P(TTMT-co-Py)/PEDOT device at voltages varying between -2.4 V and +0.6 V was shown in Figure 3.22. Upon a

stepwise increase of the applied potential from -2.4 V to +0.8 V, alternation of the color from brownish yellow to blue was observed. A maximum absorption due to π-π* transition of P(TTMT-co-Py) was observed at 380 nm, and the color of the device was dominated by the copolymer. With the application of +0.8 V, P(TTMT-co-Py) was fully oxidized whereas PEDOT was completely reduced, π-π* transition of PEDOT was monitored at 580 nm, and thus, at this voltage the color of the ECD was blue.

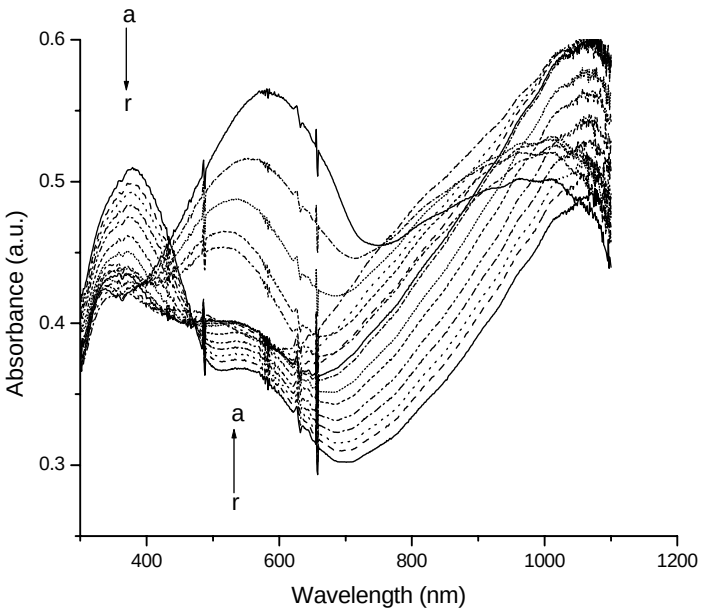

Figure 3.22 Spectroelectrochemistry of P(TTMT-co-Py)/PEDOT device as a function of wavelength at potentials between –2.4 V and +0.8 V: (a) –2.4 V, (b) -2.2 V, (c) 2.0 V, (d) -1.8 V, (e) -1.6 V, (f) -1.4 V, (g) -1.2 V, (h) -1.0 V, (i) -0.8 V, (j) -0.6 V, (k) -0.4 V, (l) -0.2 V, (m) 0.0 V, (n) +0.2 V, (o) +0.4 V, (p) +0.6 V, (r) +0.8 V.

3.3.2 Colorimetry Measurements of P(TTMT-co-Py)/PEDOT Device

When 0.0 V bias applied to the anodically coloring polymer layer the ECD has grayish red color (L = 74.4, a = 5.2, b = -9.9). Upon application of -2.4 V, greenish yellow color (L = 73.7, a = -9.7, b = 20) was observed. With the application of +0.8 V, the polymer was completely oxidized whereas the PEDOT layer was fully reduced; at this potential the color of the device was blue (L = 59, a = -2.5, b = -28.3). The different colors of the ECD were shown in Figure 3.23.

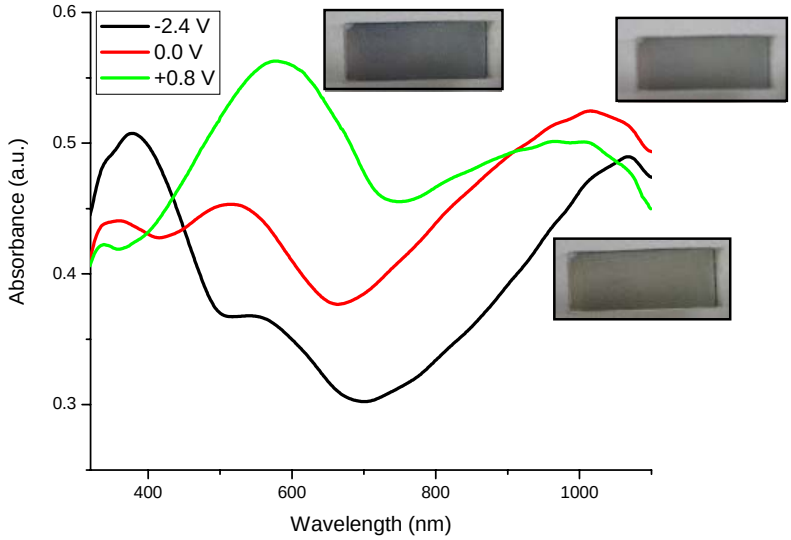

Figure 3.23 Colors of P(TTMT-co-Py)/PEDOT device at different switching voltages

3.3.3 Switching Properties of P(TTMT-co-Py)/PEDOT Device

To investigate switching characteristics of the ECD's, percent transmittance change at the maximum contrast wavelength was monitored while stepping potential between -2.4 V and +0.8 V during 140 s. For the

device, maximum contrast (%ΔT) and switching time were measured at 580 nm, and found as 17.5% and 1.6 s, respectively (Figure 3.24).

3.3.4 Open Circuit Memory of P(TTMT-co-Py)/PEDOT Device

The ECD was polarized in the brownish yellow/grayish red/blue states by an applied pulse -2.4V/0.0 V/+0.8 V respectively for 1 sec, and then kept under open circuit conditions for 199 s, while the optical spectrum at 580 nm as a function of time was monitored (Figure 3.25). As seen in the figure mentioned, upon application of 0.0 V at the end of each199 s no significant change in the percent transmittance (60.4%) was observed. When polarized upon application of +0.8 V in the blue colored state, %T suddenly changed to 52.5%, whereas during 199 s the ECD tried to reach 54% transmittance; on the other hand, upon application of -2.4 V %T changed to 49%, whereas during 199 s the ECD tried to reach 51.6% transmittance, in other words it was able to remember its color.

3.3.5 Stability of P(TTMT-co-Py)/PEDOT Device

The voltage of the device was continuously swept between –2.0 V and +2.5 V with 500 mV/s scan rate and cyclic voltammetry was monitored (Figure 3.26). As seen in the figure mentioned, P(TTMT-co-Py)/PEDOT ECD could be repeatedly switched up to 500 cycles retaining most (79%) of its electroactivity.

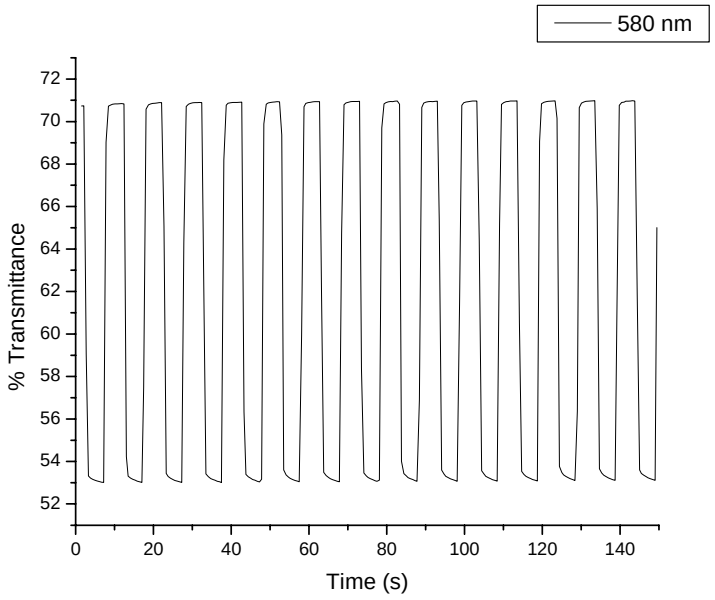

Figure 3.24 Electrochromic switching, percent transmittance change monitored at 580 nm for P(TTMT-co-Py)/PEDOT device between –2.4 V and +0.8 V.

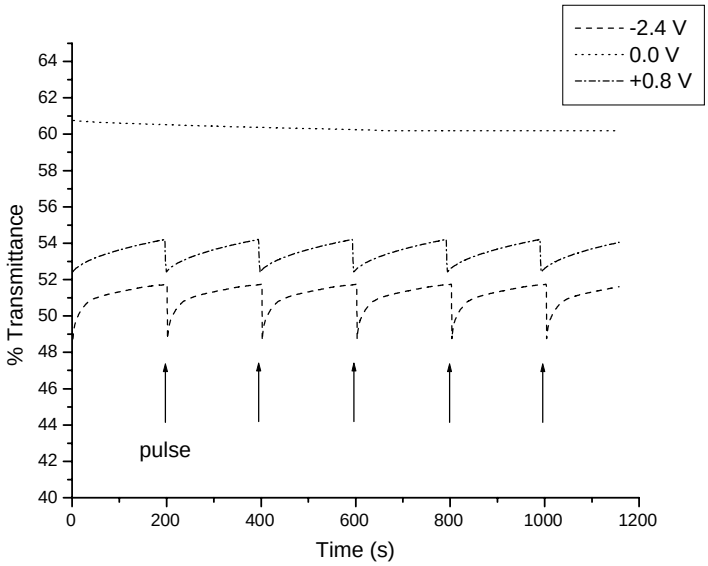

Figure 3.25 Open circuit memory of P(TTMT-co-Py)/PEDOT ECD monitored at 580 nm, pulses are applied for 1s every 200 s to recover the initial transmittance.

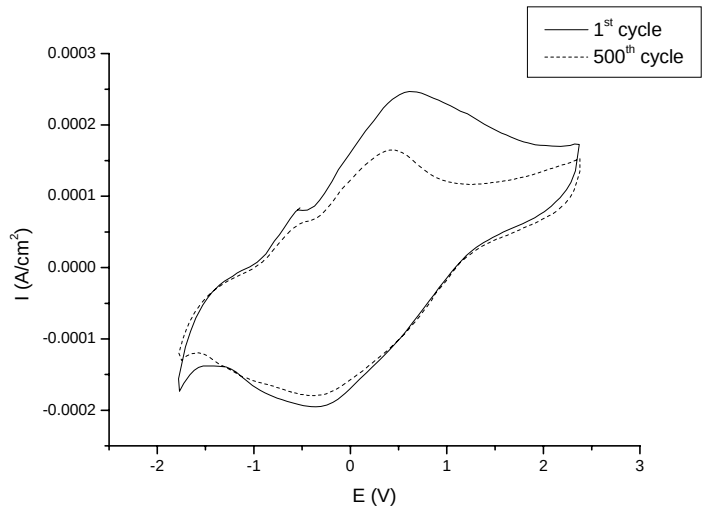

Figure 3.26 Cyclic voltammogram of P(TTMT-co-Py)/PEDOT ECD as a function of repeated scans 500 mV/s: after 1 cycle (solid line), after 500 cycles (dashed line).

3.4 Synthesis of FPTP and Its Homopolymers and Their Characterization

3.4.1 Characterization of FPTP with NMR and FTIR Spectroscopies

The structure of the monomer was confirmed by ^{1}H-NMR and ^{13}C-NMR.

^{1}H-NMR (δ, ppm) data (Figure 3.27) for FPTP: 6.48 (s, 2 H, pyrrolyl), 6.50 (d, J = 3.6 Hz, 2 H, 3-thienyl), 6.79 (dd, J = 3.8 and 4.9 Hz, 2 H, 4-thienyl), 7.01 (d, J = 5.1 Hz, 2 H, 5-thienyl), 7.03 (d, J = 8.6 Hz, 2 H, phenyl), 7.22 (multiplet due to H-F coupling, 2 H, phenyl).

^{13}C-NMR (δ, ppm) data (Figure 3.28) for FPTP: 110.00 (2 C_a), 116.07 (d, $J_{C\text{-}F}$ = 22.7 Hz, 2 C_b), 116.29 (2 C_h), 124.24 (d, $J_{C\text{-}F}$ = 8.8 Hz, 2 C_c), 124.51 (2 C_f), 126.94 (2 C_d), 130.23 (2 C_e), 131.70 (2 C_i), 134.59 (2 C_g), 162.80 (d, $J_{C\text{-}F}$ = 247.9 Hz, C_j).

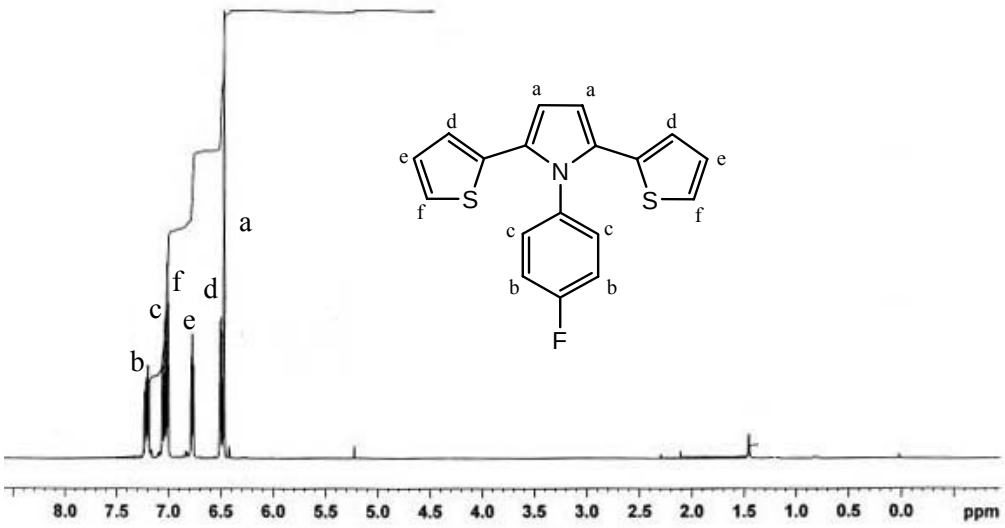

Figure 3.27 ^{1}H-NMR spectrum of FPTP

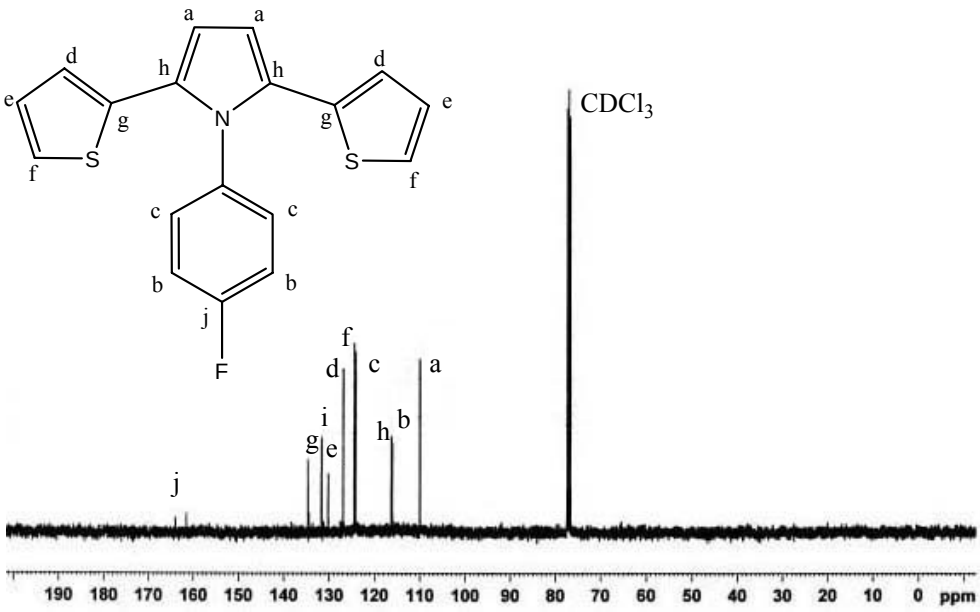

Figure 3.28 ^{13}C-NMR spectrum of FPTP

In the FTIR (Figure 3.29) spectrum of the monomer, the following peaks were identified: 693 cm^{-1} (five membered heterocyclic C-H out of plane

deformation vibration), 841 cm^{-1} (2-substituted phenyl ring, out of plane deformation vibration due two neighboring H atoms in addition to thienyl and pyrrolyl C-H_β stretching), 1034 cm^{-1} (phenyl ring, =C-H in plane deformation vibration), 1220 cm^{-1} (aromatic amine, C-N stretching vibration), 1415 cm^{-1} (C=N in plane vibration), 1458 cm^{-1} (C=C in plane vibration), 773 cm^{-1} and 3102 cm^{-1} (thienyl C-H_α stretching vibration).

Melting point of FPTP was found as 198 °C.

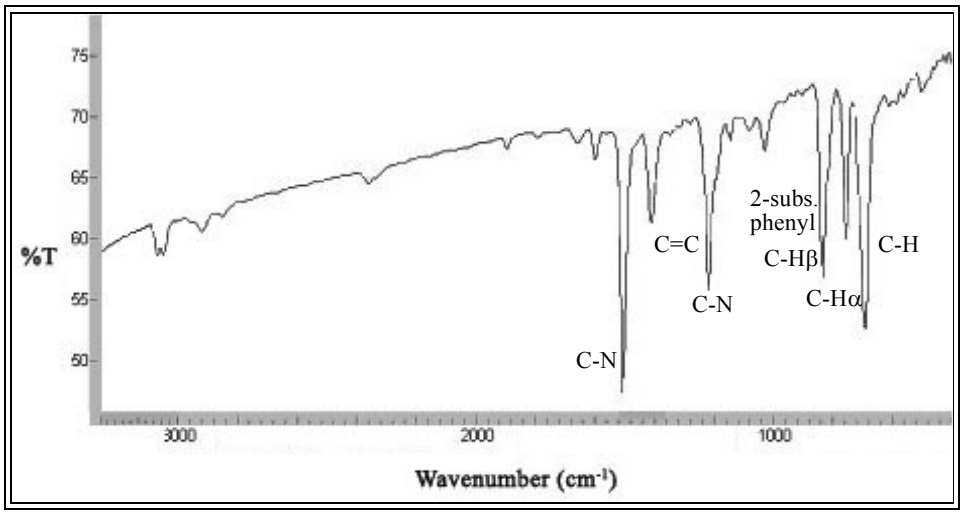

Figure 3.29 FTIR spectrum of FPTP

3.4.2 Characterization of P(FPTP) Obtained by Chemical Polymerization

3.4.2.1 ^{1}H-NMR and FTIR Spectra of P(FPTP)

The ^{1}H-NMR and FTIR spectra revealed that polymerization of FPTP was successfully realized.

^{1}H-NMR (δ, ppm) data (Figure 3.30) for P(FPTP): 6.4 ppm (broad, 2 H, pyrrolyl), 6.6 ppm (broad, 2 H, 3-thienyl), 6.8-6.9 ppm (broad, 2 H, 4-thienyl), 7.2 ppm (broad, 2 H, phenyl), 7.5 ppm (broad, 2 H, phenyl).

In the FTIR spectrum (Figure 3.31) of the polymer, most of the characteristic peaks of the monomer were retained; however, the peaks observed at 773 cm^{-1} and 3102 cm^{-1} due to thienyl C-H_α stretching vibration was completely disappeared indicating polymerization was realized from 2,5 positions of thiophenes. In addition, the shoulder observed at 1618 cm^{-1} was considered as the evidence of polyconjugation and the new peak at 694 cm^{-1} indicated the entrapment of the dopant ion, Cl^-, in the matrice.

3.4.2.2 GPC Results of P(FPTP)

Gel permeation chromatography (GPC) results revealed that number average molecular weight (Mn) was 4,545 and weight average molecular weight was 6,625 in addition, polydispersity index was calculated as 1.45. Number of repeating units was found as 15 showing that a polymeric chain was formed.

3.4.2.3 Conductivity of P(FPTP)

Room temperature (20 °C) conductivity of chemically prepared P(FPTP) was measured via a four-probe technique and determined as 0.01 S cm^{-1}.

3.4.3 Characterization of P(FPTP) Obtained by Electrochemical Polymerization

3.4.3.1 FTIR Spectrum of P(FPTP)

The FTIR spectrum revealed that electropolymerization of FPTP was successfully realized. The peaks related to C–H_α stretching of thiophene disappeared completely. The new broad band at around 1640 cm^{-1} was due to polyconjugation. The strong absorption peak at 1118, 1085 and 616 cm^{-1}

were attributed to the incorporation ClO_4^- ions into the polymer film during doping process.

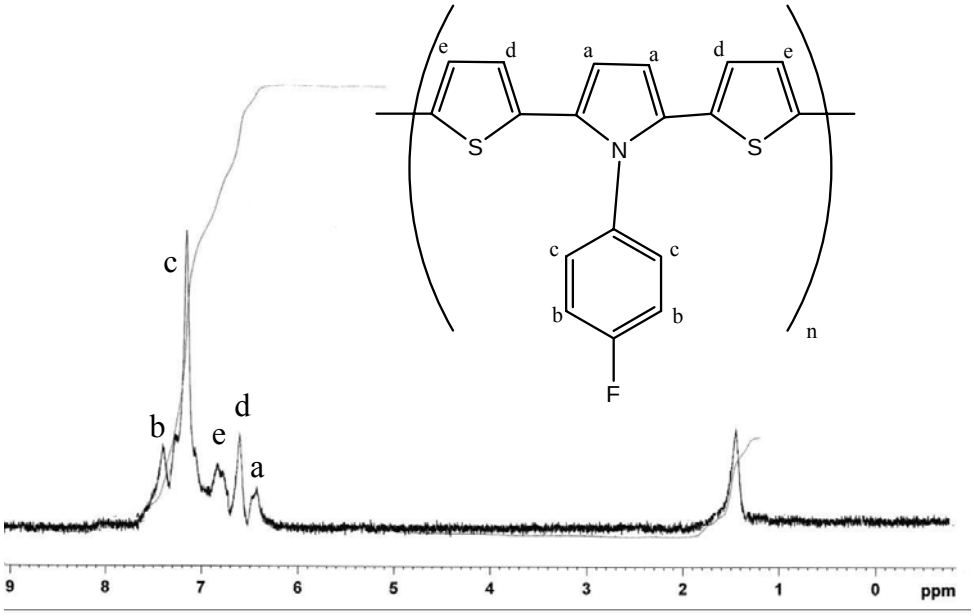

Figure 3.30 ^{1}H-NMR spectrum of chemically synthesized P(FPTP)

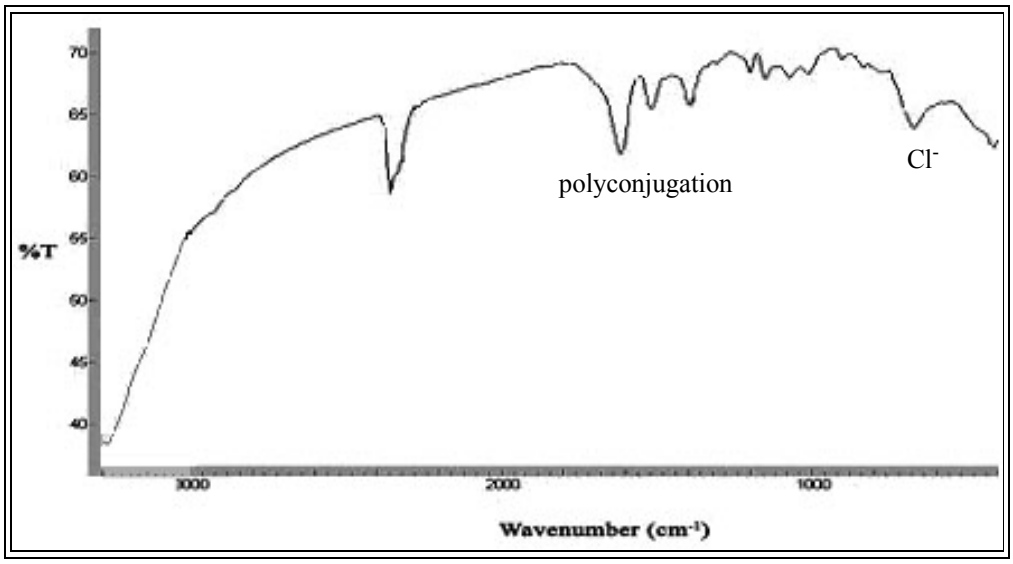

Figure 3.31 FTIR spectrum of chemically synthesized P(FPTP)

3.4.3.2 Cyclic Voltammogram of P(FPTP)

Oxidation-reduction behavior of FPTP was investigated via cyclic voltammetry. Upon sequential cycles, there was a gradual film formation, indicated by the continuous increase in the current density. In the cyclic voltammogram of P(FPTP) shown in Figure 3.32 +0.4 V and +0.6 V were observed as the oxidation peaks while +0.3 V was the reduction peak.

Figure 3.32 Cyclic voltammogram of P(FPTP)

3.4.3.3 Morphology of P(FPTP) Film

SEM micrograph of the solution side of the film synthesized electrochemically is given in Figure 3.33. The synthesized monomer exhibits homogeneous and porous structure.

3.4.3.4 Conductivity of P(FPTP) Film

Room temperature (20 °C) conductivity of electrochemically prepared P(FPTP) was measured via a four-probe technique and determined as 0.001 S cm^{-1}.

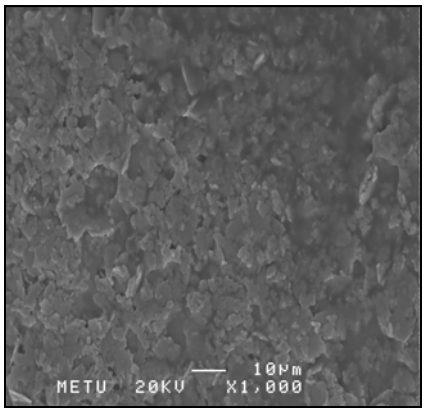

Figure 3.33 SEM picture of solution side of P(FPTP)

3.4.3.5 Spectroelectrochemistry of P(FPTP)

FPTP was polymerized onto an ITO glass electrode via potentiodynamic method in AN containing 0.10 M of $NaClO_4$ and 0.10 M of $LiClO_4$. The coated glass electrode was placed in a monomer free environment and its spectroelectrochemical properties, i.e. electronic transitions and change in optical properties upon redox switching, were determined. Optoelectrochemical spectra of the polymer as a function of applied potential are given in Figure 3.34. At the neutral state λmax value due to π-π* transition of the polymer was found to be 398 nm with a band gap of 1.94 eV. Upon applied voltage, reduction in the intensity of the π-π* transitions and formation of charge carrier bands were observed. Thus, appearance of peaks

around 510 and 850 nm could be attributed to the evolution of polaron and bipolaron bands, respectively (Figure 3.35).

3.4.3.6 Colorimetry Measurements of P(FPTP)

At the fully reduced state the color of the polymer was pale greenish yellow (L = 82, a = -11, b = 1); on the other hand, at the fully oxidized state the film has a pale bluish gray color (L = 77, a = -8, b = -18) as seen in Figure 3.36.

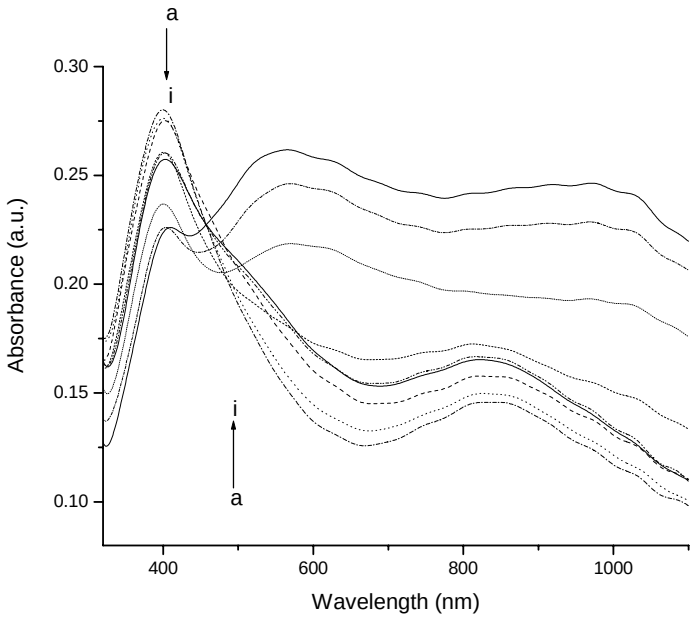

Figure 3.34 Spectroelectrochemistry of P(FPTP) as a function of wavelength (300 nm-1100 nm)at applied potentials between –0.6 and +1.0 V: (a) –0.6 V, (b) –0.4 V, (c) –0.2 V, (d) 0.0 V, (e) +0.2 V, (f) +0.4 V, (g) +0.6 V, (h) +0.8 V, (i) +1.0 V.

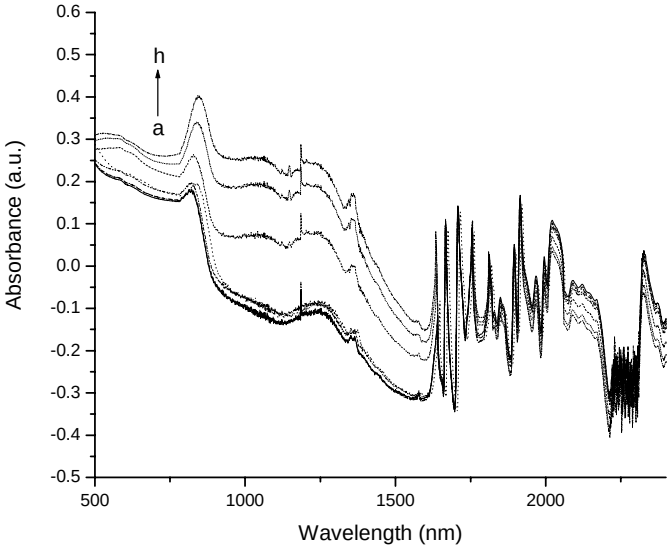

Figure 3.35 Spectroelectrochemistry of P(FPTP) as a function of wavelength (500 nm-2400 nm) at applied potentials between –0.6 V and +1.0 V: (a) –0.6 V, (b) –0.4 V, (c) 0.0 V, (d) +0.2 V, (e) +0.4 V, (f) +0.6 V, (g) +0.8 V, (h) +1.0 V.

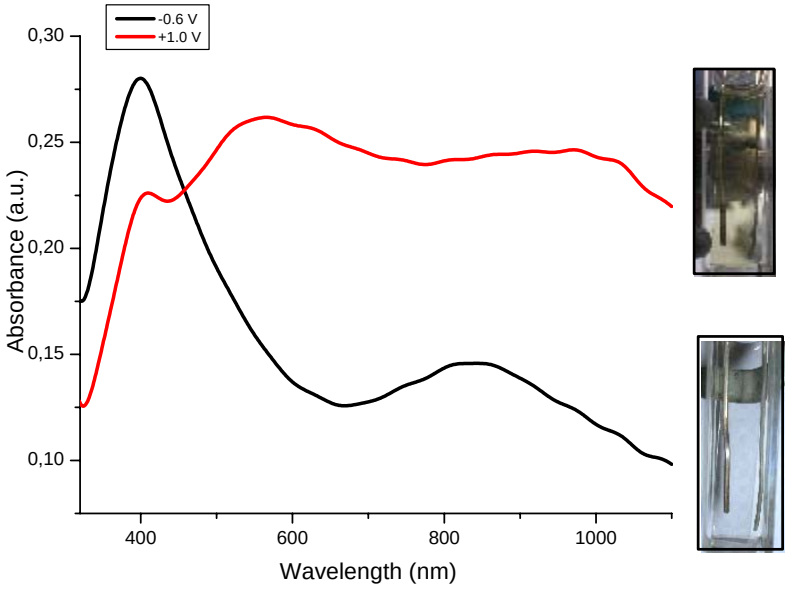

Figure 3.36 Colors of P(FPTP) at different switching voltages

3.4.3.7 Switching Properties of P(FPTP)

During the experiment, the homopolymer electrochemically coated onto ITO glass was switched between -0.6 V and +1.0 V (Figure 3.37), in other words between neutral and doped states, respectively, for five seconds. For P(FPTP), optical contrast (%ΔT) and switching time were calculated as 2.3% and 0.8 s respectively at the given λmax. However, the maximum contrast in the visible range was found as 6% at 600 nm, at that wavelength, switching time was calculated as 1.2 s.

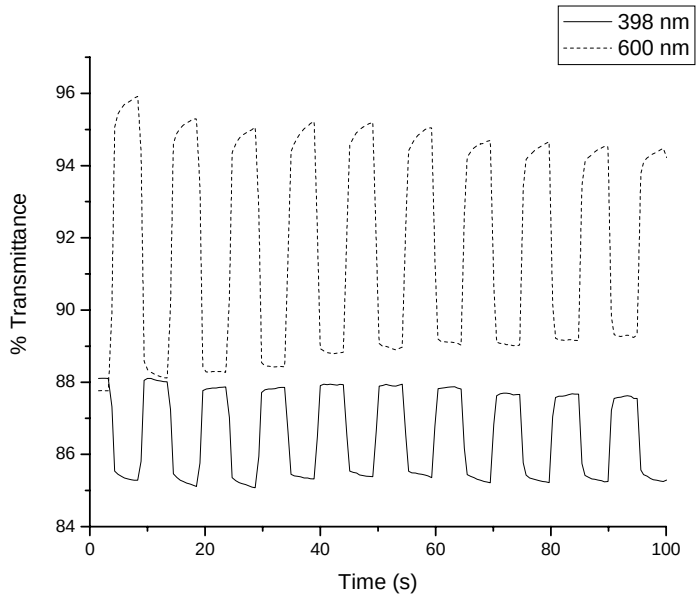

Figure 3.37 Electrochromic switching, percent transmittance change monitored at 398 nm (solid line) and 600 nm (dashed line) for P(FPTP) between –0.6 V and +1.0 V.

3.5 Characterization of P(FPTP)/PEDOT Device

3.5.1 Spectroelectrochemistry of the Device

Spectroelectrochemical studies were carried out to examine optical changes upon application of different voltages. Figure 3.38 represents the spectra of the P(FPTP)/PEDOT device recorded during application of different voltages varying between –0.8 V and +1.1 V. Upon a stepwise increase of the applied potential from –0.8 V to +1.1 V, alternation of the color from yellowish brown to blue was observed. A maximum absorption due to π to π^* transition of P(FPTP) was observed at 445 nm. At that potential, the PEDOT layer was transparent sky blue since it was in its oxidized state; as a consequence the P(FPTP) dominated the color of the ECD, which was in its reduced state. At potentials beyond +0.8 V, the PEDOT was reduced and evaluation of a new peak at around 615 nm due to π to π^* transition was monitored. With the application of +1.1 V, P(FPTP) was fully oxidized whereas PEDOT was completely reduced, and thus, at this voltage the color of the ECD was blue.

3.5.2 Colorimetric Measurements of the Device

Upon application of –0.8 V to the anodically coloring polymer layer, P(FPTP) was completely reduced and the ECD has yellowish brown color (L = 74, a = -2, b = 4). With the application of +1.1 V, the polymer was completely oxidized whereas the PEDOT layer was fully reduced; at this potential the color of the device was blue (L = 59, a = -4, b = -20). The colors of the device were shown in Figure 3.39.

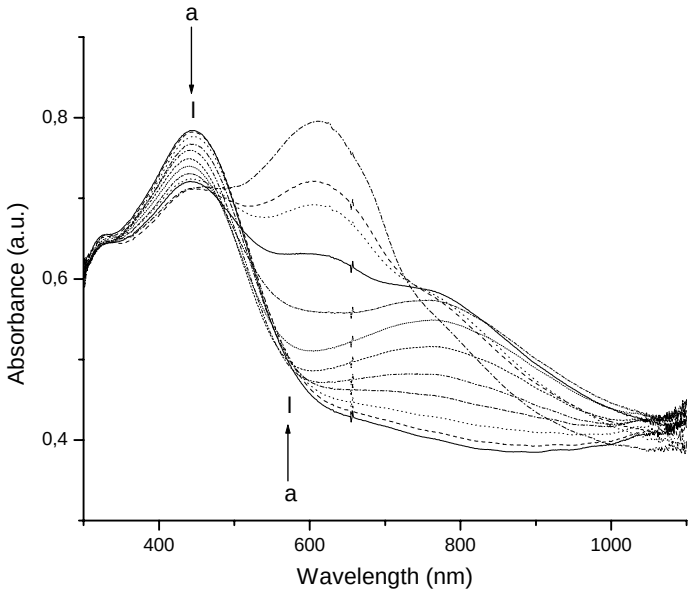

Figure 3.38 Spectroelectrochemistry of P(FPTP)/PEDOT device as a function of wavelength at potentials between –0.8 V and +1.1 V: (a) –0.8 V, (b) –0.6 V, (c) –0.4 V, (d) -0.2 V, (e) 0.0 V, (f) +0.2 V, (g) +0.4 V, (h) +0.6 V, (i) +0.8 V, (j) +0.9 V, (k) +1.0 V, (l) +1.1 V.

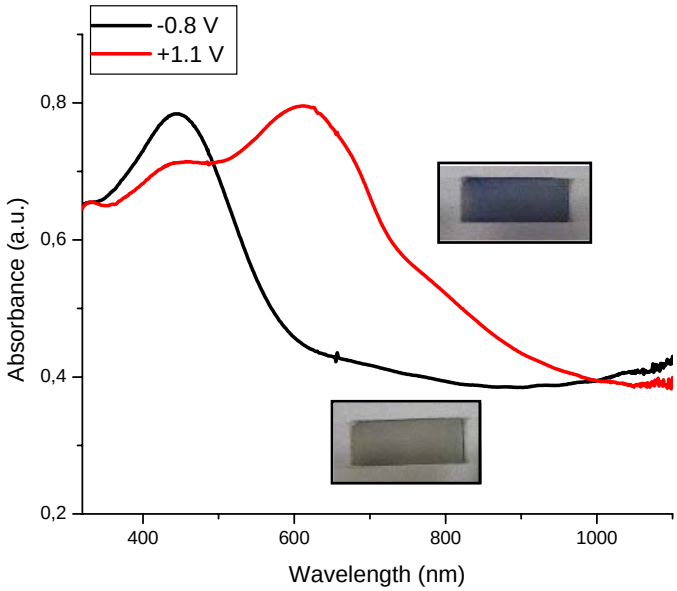

Figure 3.39 Colors of P(FPTP)/PEDOT device at different switching voltages

3.5.3 Switching Properties of the Device

In this double potential step experiment the ability of the device to switch between the two colored states with a change in optical transmittance at a fixed wavelength was tested, optical contrast as well as switching time were determined. The results were displayed in Figure 3.40 for switching time of five seconds. The maximum optical contrast was calculated as 19.4% and the switching time was found as 1.4 s at 615 nm.

3.5.4 Open Circuit Memory of the Device

In the experiment, the ECD was polarized in the yellowish brown/blue states by an applied pulse (-0.8 V/+1.1 V, yellowish brown/blue colored states, respectively) for 1 second and then kept under open circuit conditions for 199 seconds while the optical spectrum at 615 nm as a function of time was monitored (Figure 3.41). As seen in the figure mentioned, upon application of 0.0 V at the end of each 199 s no significant change in the percent transmittance (62%) was observed. On the other hand application of +1.1 V resulted in 46% transmittance whereas during 199 s the ECD tried to reach 62% transmittance, moreover when -0.8 V was applied the %T altered to 64%. As a consequence, the device was able to remember its color upon application of potential.

3.5.5 Stability of the Device

Redox stability is essential for construction of reliable electrochromic devices with long lifetimes. For this purpose non-stop cycling of the applied potential between -0.5 and +2.0 V with 500 mV/s scan rate was performed. As seen in Figure 3.42 even after 1000^{th} run the device was retaining most (88%) of its electroactivity.

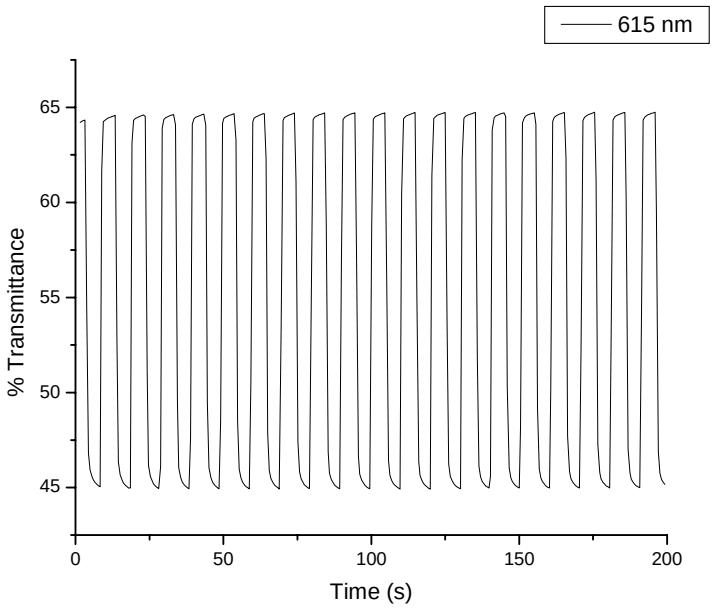

Figure 3.40 Electrochromic switching, percent transmittance change monitored at 615 nm for P(FPTP)/PEDOT ECD between –0.8 V and +1.1 V.

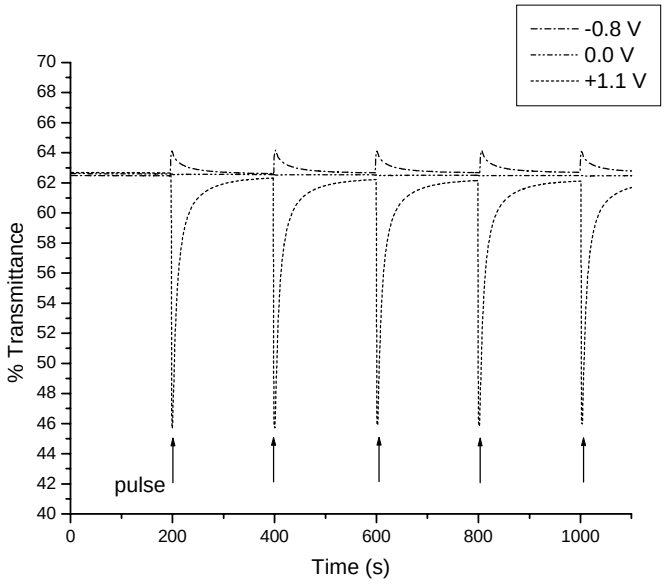

Figure 3.41 Open circuit memory of P(FPTP)/PEDOT ECD monitored at 615 nm, pulses are applied for 1s every 200 s to recover the initial transmittance.

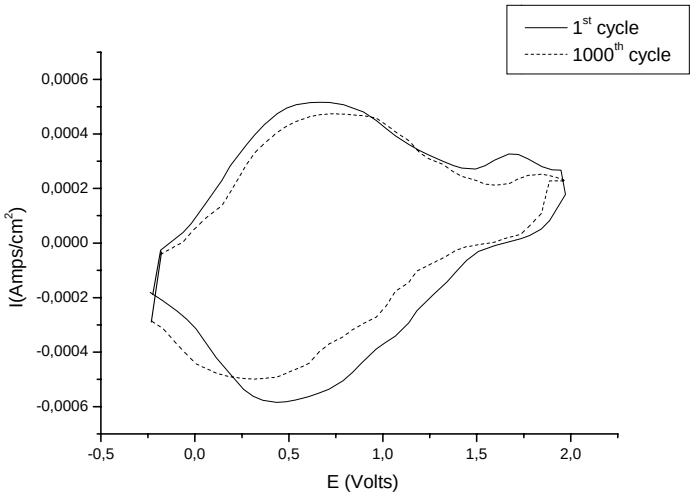

Figure 3.42 Cyclic voltammogram of P(FPTP)/PEDOT ECD as a function of repeated scans 500 mV/s: after 1 cycle (solid line), after 1000 cycles (dashed line).

CHAPTER IV

CONCLUSION

Synthesis of terephthalic acid bis-(thiophen-3-ylmethyl)thioester (TTMT), and its copolymers with thiophene and pyrrole were successfully accomplished. Optoelectronic and switching properties of P(TTMT-co-Th) and P(TTMT-co-Py) were investigated. Spectroelectrochemistry experiments showed that π to π^* transition occurs at 476 nm with a band gap 2.0 eV for P(TTMT-co-Th), on the other hand λmax of P(TTMT-co-Py) was found as 375 nm and the band gap was calculated as 2.4 eV.

P(TTMT-co-Th)/PEDOT and P(TTMT-co-Py) electrochromic devices were assembled in sandwich configuration: ITO coated glass/anodically coloring polymer [P(TTMT-co-Th)] or [P(TTMT-co-Py)]||gel electrolyte||cathodically coloring polymer (PEDOT)/ITO coated glass. The P(TTMT-co-Th)/PEDOT device color changed between brown and blue upon application of potential. The switching voltages were 0.0 V and +2.6 V, switching time and optical contrast were found as 1.1 s and 11%, respectively. The ECD showed optimal redox stability and optical memory under atmospheric conditions. P(TTMT-co-Py)/PEDOT device has a three different colors; brownish yellow, grayish red and blue upon application of different potentials. The switching voltages were -2.4 V and +0.8 V, switching time and optical contrast were found as 1.6 s and 17.5%, respectively. As the P(TTMT-co-Th)/PEDOT ECD, this ECD also showed optimal redox stability and optical memory under atmospheric conditions.

A fully conjugated new monomer, called as 1-(4-fluorophenyl)-2, 5-di(thiophen-2-yl)-1*H*-Pyrrole (FPTP)was successfully synthesized and it was chemically as well as electrochemically polymerized. Since the chemically produced homopolymer of this new thiophene functionalized monomer was soluble in some organic solvents, NMR and GPC were utilized to characterize it. Spectroelectrochemistry as well as switching properties of the electrochemical homopolymer of FPTP were investigated. Spectroelectrochemistry experiments showed that π to π^* transition occurred at 398 nm, furthermore band gap energy was calculated as 1.94 eV. P(FPTP)/PEDOT electrochromic device was assembled in sandwich configuration: ITO coated glass/anodically coloring polymer [P(FPTP)]||gel electrolyte||cathodically coloring polymer (PEDOT)/ITO coated glass. The device color changed between yellowish brown and blue upon application of –0.8 V and +1.1 V, respectively. Switching time and optical contrast were found as 1.4 s and 19.4% at maximum contrast point, respectively. The ECD showed optimal redox stability and optical memory under atmospheric conditions.

REFERENCES

1. V.V. Walatka, M. M. Labes, and J. H. Perlstein**,** *Phys. Rew. Lett*. **31,** p.1139, 1973.

2. H. Shirakawa, E.J. Louis, A.G. MacDiarmid, C.K. Chiang, A.J. Heeger, *J. Chem. Soc., Chem. Commun.* p.578, 1977.

3. C.K. Chiang, C.R. Fischer, Y.W. Park, A.J. Heeger, H. Shirakawa, E.J. Louis, S.C. Gau, A.G. MacDiarmid, *Phys. Rev. Lett.* **39**, p.1098, 1977.

4. H. Shirakawa, in *Handbook of Conducting Polymers, 2nd ed*.; T.A. Skotheim, R.L. Elsenbaumer, J.R. Reynolds, Eds.; Marcel Dekker, New York, 1998, pp.197-208.

5. J.C.W. Chien, *Polyacetylene: Chemistry, Physics, and Materials Science, Academic,* Orlando, 1984.

6. A. Heeger, *Rev. Mod. Phys.* **73**, pp.681-682, 2001.

7. G. L. Miessler, D. A. Tarr, *Inorganic Chemistry 2nd ed*., New Jersey, 1999.

8. C. K. Chiang, M. A. Druy, S. C. Gau, A. J. Heeger, E. J. Louis, A. G. MacDiarmid, *J. Am. Chem. Soc*. **100**, p.1013, 1978.

9. A. G. MacDiarmid, *Synth. Met*. **125**, p.12, 2002.

10. K. E. Ziemelis, A. T. Hussain, D. D. C. Bradley, R. H. Friend, J. Rilhe, G. Wegner, *Phys. Rev. Lett*. **66**, p.2231, 1991.

11. P. J. Nigrey, A. G. MacDiarmid, A. J. Heeger, *J. Chem. Soc. Chem. Commun*., p.594, 1979.

12. D. MacInnes Jr., M. A. Druy, P. J. Nigrey, D. P. Nairns, A. G. MacDiarmid, A. J. Heeger, *J. Chem. Soc. Chem. Commun*., p.317, 1981.

13. D. Kumar, R. C. Sharma, *Eur. Polym. J.* **34**, pp.1053-1060, 1998.

14. A. Malinauskas, *Polymer*. **42**, p.3958, 2000.

15. N. Toshima, S. Hara, *Prog. Polym. Sci.* **20**, p.164, 1995.

16. R. J. Mortimer, A. L. Dyer, J. R. Reynolds, *Displays* **27**, pp.2-14, 2006.

17. J. Roncali, *Chem. Rev.* **92**, pp.711-738, 1992.

18. J.R. Reynolds, J.P. Ruiz, A.D. Child, K. Navak, D.S. Marynick, *Macromolecules* **24**, p.678, 1991.

19. J.R. Reynolds, A.D. Child, J.P. Ruiz, S.Y. Hong, D.S. Marynick, *Macromolecules* **26**, p.2095, 1993.

20. D. Zhang, J. Qin, G. Xue, *Synthetic Metals* **100**, pp.285-289, 1999.

21.G. Shi, S. Jin, G. Xue, C. Li, *Science* **267**, p.994, 1995.

22. S. Jin, G. Xue, *Macromolecules* **30**, pp.5753-5757, 1997.

23. F. Selampınar, U. Akbulut , T. Yılmaz, A. Gungor, L. Toppare, *J. of Polym. Sci:Part A Polym.Chem.* **35**, pp.3009-3016, 1997.

24. H. Koezuka, S. Etoh, J. *Appl. Phys.* **54**, p.2511, 1983.

25. K. K. Kanazawa, A. F. Diaz, W. Will, P. Grant, G. B. Street, G. P. Gardini, G. Kwak, *Synth.Met.* **1**, p.320, 1980.

26. S. Kuwabata, S. Ito, H. Yoneyama, *J. Electrochem. Soc.* **135**, p.1691, 1988.

27. O. Inganas, B. Liedberg, W. Hang-Ru, H. Wynberg, *Synth. Met.* **11**, p.239, 1985.

28. J. P. Ferraris, G. D. Skiles, *Polymer* **28**, p.179, 1987.

29. O. Niva, T. Tamamura, M. Kakuchi, *Macromolecules* **20**, p.749, 1987.

30. M. A. DePaoli, R. J. Waltman, A. F. Diaz and I. Bargon, *J. Polym. Sci. Polym. Chem. Ed.* **23**, p.1687, 1985.

31. G. Nagausubramanian, S. DiStefano, *I. Electrochem. Soc. Extended Abstr.* **85-2**, p.659, 1985.

32. H. L. Wang, L. Toppare and J. F. Fernandez, *Macromolecules* **23**, p.1053, 1990.

33. D. Stanke, M. L. Hallensleben, L. Toppare, *Synth. Met.* **55**, p.1108, 1988.

34. D. Stanke, M. L. Hallensleben, L. Toppare, *Macromol. Chem. Phys.* **196**, p.1697, 1988.

35. D. Stanke, M. L. Hallensleben, L. Toppare, *Synth. Met.* **73**, p.261, 1995.

36. F. Selampmar, U. Akbulut, T. Yilmaz, A. Gürgör, L. Toppare, I. *Polym. Sci. Polym. Chem.* **5**, p.3009, 1997.

37. F. Selampınar, U. Akbulut, T. Yalçın, S. Süzer, L. Toppare, *Synth. Met.* **62**, p.201, 1999.

38. F. Kalaycioglu, L. Toppare, *Y.* Yagci, V. Harabagiu, M. Pintela, R. Ardelean, B. Simunescu, *Synth. Met.* **97**, p.7, 1998.

39. N. Kizilyar, L. Toppare, A. Onen, Y. Yagci, *Polym. Bull.* **40**, p.639, 1997.

40. S. Oztemiz, L. Toppare, A. Önen, Y. Yağci, *JMS-Pure Appl.Chem.* **A37**, p.277, 2000.

41. O. Turkarslan, A. Erden, E. Sahin, L. Toppare, *J. Macr. Sci*. **43**, pp.115-128, 2006.

42. P. Camurlu, A. Cirpan; L. Toppare, *J. Electroanal. Chem.* **572**, pp.61-65, 2004.

43. Y. Coskun, A. Cirpan, L. Toppare, *Polymer*. **45**, pp.4989-4995, 2004.

44. P. Camurlu, A. Cirpan, L. Toppare, *Synth. Met.* **146**, pp.91-97, 2004.

45. G. Sonmez, C. K. F. Shen, Y. Rubin, F. Wudl, Angew. *Chem. Int. Ed.* **43**, pp.1497-1502, 2004.

46. C. J. DuBois, F. Larmat, D. J. Irvin, J. R. Reynolds, *Synth. Met.* **119**, pp. 321-322, 2001.

47. A. Cirpan, H. P. Rathnayake, G. Gunbas, P. M. Lahti, F. E. Karasz, *Synth. Met.*, **156**, pp.282-286, 2006.

48. A. Cirpan, L. Ding, F. Karasz, *Synth. Met.* **150**, pp.195-198, 2005.

49. L. Kumar, S. K. Dhawan, M. N. Kamalasanan, S. Chandra, *Thin Solid Films* **441**, pp.243-247, 2003.

50. S. Kiralp, L. Toppare, Y. Yağcı, *Synth. Met.* **135-136**, pp.79-80, 2003.

51. H. B. Yildiz, S. Kiralp, L. Toppare, Y. Yagci, *React. Funct. Polym.* **65**, pp.343-350, 2005.

52. W. J. Sung, Y. H. Bae, *Sensor. Actuat. B-Chem.* **114**, pp.164-169, 2006.

53. M. K. Ram, Ö. Yavuz, M. Aldissi, *Synth. Met.* **151**, pp.77-84, 2005.

54. M. K. Ram, Ö. Yavuz, V. Lahsangah, M. Adissi, *Sensor. Actuat. B-Chem.* **106**, pp.750-757, 2005.

55. E. Arici, H. Hoppe, F. Schaffler, D. Meissner, M. A. Malik, N. S. Sarıçiftçi, *Thin Solid Films* **451-452**, pp.612-618, 2004.

56. H. Hoppe, N. Arnold, D. Meissner, N. S. Sarıçiftçi, *Thin Solid Films* **451-452**, pp.589-592, 2004.

57. H. K. Kim, M. S. Kim, K. Song, Y. H. Park, S. H. Kim, J. Joo, J. Y. Lee, *Synth. Met.* **135-136**, pp.105-106, 2003.

58. M. S. Lee, H. S. Kong, J. Joo, A. J. Epstein, J. Y. Lee, *Thin Solid Films* **477**, pp.169-173, 2005.

59. K. S. Ryu, Y. Lee, K. S. Han, M. G. Kim, *Mater. Chem. Phys.* **84**, pp.380-384, 2004.

60. M. A. De Paoli, W. A. Gazotti, *J. Braz Chem. Soc.***13**, pp.410-424, 2002.

61. S. H. Kim, J. S. Bae, S. H. Hwang, T. S. Gwon, M. K. Doh, *Pigments* **33**, pp.167-172, 1997.

62. A. Pennisi, F. Simone, G. Barletta, G. Di Marco, M. Lanza, *Electrochim. Acta* **44**, pp.3237-3243, 1999.

63. N. Ozer, C. M. Lampert, *Thin Solid Films* **349**, pp.205-211, 1999.

64. C. O. Avellaneda, P. R. Bueno, R. C. Faria, L. O. S. Bulhoes, *Electrochim. Acta* **46**, pp.1977-1981, 2001.

65. Y. H. Huang, L. C. Chen, K. C. Ho, *Solid State Ionics* **165**, pp.269-277, 2003.

66. C. L. Lin, C. C. Lee, K. C. Ho, *J. Electroanal. Chem.* **524-525**, pp.81-89, 2002.

67. R. Jones, A. Krier, K. Davidson, *Thin Solid Films* **298**, pp.228-236, 1997.

68. T. A. Skotheim, R. L. Elsenbaumer, J. R. Reynolds, *Handbook of Conducting Polymers, 2nd ed*., Marcel Dekker, New York, 1998.

69. J. Roncali, *Chem Rev.* **97**, pp.173-205, 1997.

70. P. R. Somani, S. Radhakrishnan, *Mater. Chem. Phys.* **77**, pp.117-133, 2002.

71. A. A. Argun, P. H. Aubert, B. C. Thompson, I. Schwendeman, C. L. Gaupp, J. Hwang, N. J. Pinto, D. B. Tanner, A. G. MacDiarmid, J. R. Reynolds, *Chem. Mater.* **16**, pp.4401-4412, 2004.

72. E. Campaigne, W. M. LeSuer, *J. Am. Chem. Soc*. **70**, pp.1555-1558, 1948.

73. P. Cagniant, D. Cagniant, *Bull. Soc. Chim. Fr.* **7**, pp.2597-2605, 1967.

74. A. Merz, F. Ellinger, *Synthesis.* **6**, p.42, 1991.

75. J. Nakazaki, I. Chung, M. M. Matsushita, T. Sugawara, R. Watanabe, A. Izuoka, Y. J. Kawada, *Mater. Chem.* **13**, pp.1011-1022, 2003.

76. K. Ogura, R. Zhao, H. Yanai, K. Maeda, R. Tozawa, S. Matsumoto, M. Akazome, *Bull. Chem. Soc. Jpn.* **75**, pp.2359-2370, 2002.

77. P. E. Just, I. Chane-Ching, P. C. Lacaze, *Tetrahedron* **58**, pp.3467-3472, 2002.

78. E. M. Girotto, M. A. DePaoli, *J. Braz. Chem. Soc.* **10**, pp.394-400, 1999.

79. W. A. Gazotti, G. Casalbore-Micelli, A. Geri, M. A. DePaoli, *Adv. Mater.* **10**, pp.60-64, 1998.

80. A. F. Diaz, A. Martinez, K. K. Kanazawa, M. M. Salmon, *J. Electroanal. Chem.* **130**, p.181, 1980.